A COMPARISON BETWEEN LOW-DOSE AND STANDARD DOSE NON-CONTRAST MULTIDETECTOR COMPUTED TOMOGRAPHIC IMAGING IN INFLAMMATORY DISEASES OF PARANASAL SINUSES

By
Dr. Rajkumar.R

SDUAHER

DISSERTATION SUBMITTED TO SRI DEVARAJ URS ACADEMY OF HIGHER EDUCATION AND RESEARCH, KOLAR, KARNATAKA

In partial fulfillment of the requirements for the degree of

DOCTOR OF MEDICINE
IN
RADIODIAGNOSIS

Under the Guidance of
Dr. ANIL KUMAR SAKALECHA., MD(RD).,
Professor
&
Co-Guidance of
DR.AZEEM MOHIYUDDIN., MS (Otorhinolaryngology).,
Professor

DEPARTMENT OF RADIODIAGNOSIS,
SRI DEVARAJ URS MEDICAL COLLEGE & RESEARCH CENTER,
TAMAKA, KOLAR-563101

MAY 2015

DECLARATION BY THE CANDIDATE

I hereby declare that this dissertation/thesis entitled **"A COMPARISON BETWEEN LOW-DOSE AND STANDARD DOSE NON-CONTRAST MULTIDETECTOR COMPUTED TOMOGRAPHIC IMAGING IN INFLAMMATORY DISEASES OF PARANASAL SINUSES"** is a bonafide and genuine research work carried out by me under the guidance of **Dr.ANILKUMAR SAKALECHA** M.D(R.D), Professor Department of Radiodiagnosis, Sri DevarajUrs Medical College Tamaka, Kolar.

Date:

Place: Kolar

Dr. RAJKUMAR.R
Post Graduate.
Department of Radiodiagnosis.
Sri Devaraj Urs Medical College and
Research Centre, Tamaka
Kolar

CERTIFICATE BY THE GUIDE

This is to certify that the dissertation entitled **"A COMPARISON BETWEEN LOW-DOSE AND STANDARD DOSE NON-CONTRAST MULTIDETECTOR COMPUTED TOMOGRAPHIC IMAGING IN INFLAMMATORY DISEASES OF PARANASAL SINUSES"** is a bonafide research work done by **Dr. RAJKUMAR R,** under my direct guidance and supervision at Sri DevarajUrs Medical College and Research Center, Kolar**,** in partial fulfillment of the requirement for the degree of "**M.D. IN RADIODIAGNOSIS"**.

Date:

Place: Kolar

Dr. ANILKUMAR SAKALECHA, MD
Professor
Department Of Radiodiagnosis
Sri Devaraj Urs Medical College and
Research Center, Tamaka
Kolar

CERTIFICATE BY THE CO- GUIDE

This is to certify that the dissertation entitled "**A COMPARISON BETWEEN LOW-DOSE AND STANDARD DOSE NON-CONTRAST MULTIDETECTOR COMPUTED TOMOGRAPHIC IMAGING IN INFLAMMATORY DISEASES OF PARANASAL SINUSES**" is a bonafide research work done by **Dr. RAJKUMAR R**, under my co-guidance and supervision at **Sri Devaraj Urs Medical College and Research Center, Kolar,** in partial fulfillment of the requirement for the degree of **"M.D. IN RADIODIAGNOSIS"**.

Date:

Place: Kolar

DR.AZEEM MOHIYUDDIN.,MS
PROFESSOR,
Department Of Otorhinolaryngology And Head & Neck Surgery,
Sri Devaraj Urs Medical College and Research Center,Tamaka
Kolar

ENDORSEMENT BY THE HOD

This is to certify that the dissertation entitled **"A COMPARISON BETWEEN LOW-DOSE AND STANDARD DOSE NON-CONTRAST MULTIDETECTOR COMPUTED TOMOGRAPHIC IMAGING IN INFLAMMATORY DISEASES OF PARANASAL SINUSES"** is a bonafideresearch work done by **Dr. RAJKUMAR.R,** under the guidance of and supervision of **Dr.ANIL KUMAR SAKALECHA** at Sri DevarajUrs Medical College & Research Center, Kolar**,** in partial fulfillment of the requirement for the degree of "**M.D. IN RADIODIAGNOSIS"**.

Date:

Place: Kolar

Dr. PURNIMA HEGDE, MD
Professor and HOD
Department Of Radiodiagnosis
Sri DevarajUrs Medical College and
Research Center, Tamaka
Kolar

ENDORSEMENT BY HEAD OF THE INSTITUTION

This is to certify that the dissertation entitled "**A COMPARISON BETWEEN LOW-DOSE AND STANDARD DOSE NON-CONTRAST MULTIDETECTOR COMPUTED TOMOGRAPHIC IMAGING IN INFLAMMATORY DISEASES OF PARANASAL SINUSES"** is a bonafide research work done by **Dr. RAJKUMAR.R** under the direct guidance and supervision of **Dr. ANIL KUMAR SAKALECHA,** professor Department of Radiodiagnosis, Sri DevarajUrs Medical College, Kolar, in partial fulfillment of University regulation for the award of "**M.D. DEGREE IN RADIODIAGNOSIS**"**.**

Dr. PURNIMA HEGDE. MD,
Professor & HOD
Department Of Radiodiagnosis,
Sri DevarajUrs Medical College,
Tamaka, Kolar

Date
Place : Kolar

Dr. M.B.SANIKOP
Principal,
Sri DevarajUrs Medical College
Tamaka, Kolar

Date
Place : Kolar

COPY RIGHT

DECLARATION BY THE CANDIDATE

I, hereby declare that the Sri Devaraj Urs Academy of Higher Education and Research, Kolar, Karnataka, shall have the right to preserve, use and disseminate this dissertation / thesis in print or electronic format for academic/research purpose.

Date: **Dr. RAJKUMAR.R**

Place: Kolar

ACKNOWLEDGEMENT

I owe debt and gratitude to my parents ***Shri RAJASEKARAN and Smt. MENAKA DEVI****, along with my sister* ***Dr.ABINAYA*** *for their moral support and constant encouragement during the study.*

With humble gratitude and great respect, I would like to thank my teacher, mentor and guide, ***Dr. ANIL KUMAR SAKALECHA,*** *Professor, Department of Radiodiagnosis, Sri Devaraj Urs Medical College and Research Institute, Kolar, for his able guidance, constant encouragement, immense help and valuable advices which went a long way in moulding and enabling me to complete this work successfully.*

My sincere thanks to my co-guide ***Dr. AZEEM MOHIYUDDIN****, Professor, Department Of Otorhinolaryngology And Head & Neck Surgery ,Sri Devaraj Urs medical College, without whom, my study would not have been possible.*

I have great pleasure in expressing my deep sense of gratitude to ***Dr. PURNIMA HEGDE,*** *Professor and Head, Department of Radiodiagnosis, Sri Devaraj Urs Medical College and Research Institute, Kolar, without whose initiative and constant encouragement this study would not have been possible. Her vast experience, knowledge, able supervision and valuable advices have served as a constant source of inspiration during the entire course of my study.*

I would like to express my sincere thanks to ***Dr. PATTIBHARAMAN,*** *Professor, Department of Radiodiagnosis, Sri Devaraj Urs Medical College for his valuable support, guidance and encouragement throughout the study.*

I would like to thank ***Dr. KISHORE KUMAR, Dr .NAVINKUMAR, Dr.MUNIRATHNA. and Dr.ASHWATHNARAYANASWAMY,*** *Professors, Department of Radiodiagnosis, Sri Devaraj Urs Medical College and Research Institute, Kolar, for their constant guidance and encouragement during the study period.*

I also thank ***Dr. NAGARAJ, Dr. MANJUNATH ,Dr. NAVEEN G NAIK, Dr.JAGADISH, Dr.VINAY KK and Dr. KUKU MARIAM SURESH,*** *Assistant professors, Department of Radiodiagnosis, Sri Devaraj Urs Medical College, Kolar for their support.*

I will be falling short of my duties if I don't remember and thank ***Dr.BASHEER****, who is sadly not among us today but had always been an encouragement to all us.*

I am thankful to my fellow ***colleagues****, for having rendered all their co-operation and help to me during my study. My sincere thanks to* ***Ms.Veena*** *along with rest of the* ***staff's*** *and* ***Mr.Chandrasehar****,* ***Mr. Aleem, Mr.Mateen, Ms.Niveditha, Mr. Gurumoorthi, Mrs.Vimala*** *along with rest of the technicians of Department of Radiodiagnosis, Sri DevarajUrs Medical College and Research Institute, Kolar.*

My sincere thanks to all the patients and their families who formed the backbone of this dissertation. My sincere thanks to the Principal, SDUMC, KOLAR and the Medical Superintendent, R.L. Jalappa Hospital and Research centre (affiliated to SDUMC).

Last but not least I would be failing in my duty if I do not express my gratefulness to the almighty who has helped me to successfully complete this study.

Dr. RAJKUMAR.R

LIST OF ABBREVIATIONS

CT	**– Computed Tomography**
CTDI	**– Computed Tomography Dose index**
CTDI vol	**- Computed Tomography Dose index Volume**
DLP	**– Dose length Product**
EBCT	**– Electron Beam Computed Tomography**
mAs	**– Milli ampere seconds**
MDCT	**– Multidetector Computed Tomography**
mGy	**– Milli Gray**
MRI	**– Magnetic Resonance Imaging**
mSv	**– Milli Sieverts**
OMU	**– Osteomeatal Unit**

ABSTRACT

Background: Sinusitis is one of the most common health care problems worldwide and there is evidence that it is increasing in prevalence. Computed tomography (CT) is the gold standard for diagnosis and grading the severity of sinusitis.

Aims and Objectives: To evaluate the image quality of low-dose MDCT scanning of the paranasal sinuses and to compare image quality and effective radiation dose with low-dose and standard-dose CT protocol for paranasal sinuses.

Methodology: The prospective study was conducted in 60 patients with clinically suspected paranasal sinusitis from January 2013 to June 2014. Alternate patients were taken up for low dose MDCT (130 kV and 40 mAs) and standard dose MDCT (130 kV and 60 mAs) of the paranasal sinuses and diagnostic image quality was assessed by using a semiquantitative scoring for six anatomical structures and visualization of pathological processes. Scores of 0, 1 and 2 were assigned for structures not demonstrated, demonstrated but not clearly visualized and clearly visualized respectively. The effective dose of the scan was calculated by multiplying the dose length product with a factor of 0.0023.

Results: The baseline demographic data was similar in both the groups. The maxillary sinus was the most common sinus involved across both the study groups (86.7% each). Similar outcomes in terms of maximum scores achieved (29 patients vs 30 patients in low-dose and regular-dose group respectively; P = 0.492). Mean effective dose was 0.26

mSv (<0.36 mSv) and 0.38 mSv (>0.36 mSv) in low-dose and regular-dose group respectively.

Conclusion: Low-dose CT protocol has similar efficacy but lower radiation exposure in evaluation of paranasal sinuses for sinusitis when compared with standard-dose CT protocol. The results strongly support the role of low-dose CT for evaluation of clinically suspected sinusitis.

TABLE OF CONTENTS

LIST OF TABLES

LIST OF FIGURES

LIST OF GRAPHS

INTRODUCTION

Sinusitis is one of the most common health care problems worldwide and there is evidence that it is increasing in prevalence.

Computed tomography (CT) is the gold standard for investigation of inflammatory sinus disease and has become a routine radiologic examination in the diagnosis and grading the severity of sinusitis[1].

Conventional radiographic examinations have limited role in evaluation of sinusitis. The exquisite resolution delivered by CT comes at a price of higher radiation dose, particularly to such radiation sensitive structures such as lens and thyroid gland[2].

Limiting and reducing the radiation exposure to the eye is important, especially in young patients and in patients who require repeated scanning. There is considerable potential for reducing radiation dose for CT of the paranasal sinuses, especially if only bone structures have to be assessed.

Many investigators have discussed the possibility to perform a diagnostic CT examination of the paranasal sinuses requiring a lower radiation exposure, but still delivering the necessary information to the referring clinician.

AIMS AND OBJECTIVES

1. To study the image quality of low-dose MDCT scanning of the paranasal sinuses.

2. To compare the image quality of low-dose to the standard-dose protocol in MDCT scanning of the paranasal sinuses.

3. To compare the effective radiation dose of low-dose to the standard-dose protocol in MDCT scanning of the paranasal sinuses.

REVIEW OF LITERATURE

ANATOMY OF PARANASAL SINUSES

Embryologically nose and paranasal sinuses are interlinked. Development of head and neck along with face, nose and paranasal sinuses takes place simultaneously in a short time span. At the end of 4^{th}week embryo gets its first identifiable head and face with an orifice in its middle known as the stomodeum. The stomodeum is limited superiorly by the presence of frontonasal eminence and inferiorly by the mandibular arch. The frontonasal process forms the nasal cavity, primitive choana and nasal septum. The oronasal membrane is fully formed by the end of 5^{th}week of development. It gives rise to the floor of the nose (palate develops from this membrane).

At about 25 – 28 weeks of gestation, three medially directed projections arise from the lateral wall of the nose. This serves as the beginning of the development of paranasal sinuses.

The medial projections arising from the lateral wall of the nose forms the following structures:

1. The anterior projection forms the aggernasi
2. The inferior (maxilloturbinate) projection forms the inferior turbinate and maxillary sinus.
3. The superior projection (ethmoido turbinate) forms the superior turbinate, middle turbinate, ethmoidal air cells and their corresponding drainage channels. The middle meatus develops between the inferior and middle turbinates. The middle meatus invaginates laterally to form the embryonic infundibulum and uncinate process.

The maxillary sinus (antrum of Highmore) is the first to develop. These structures are usually fluid-filled at birth. The growth of these sinuses is biphasic with growth during years 0-3 and 7-12. During the later phase pneumatization spreads more inferiorly as the permanent teeth take their place.

The frontal sinus may develop as a direct continuation of embryonic infundibulum and frontal recess superiorly during the 16thweek. It can also develop by upward migration of anterior ethmoidal air cells to penetrate the inferior aspect of the frontal bone between its outer and inner tables.

Pneumatization of frontal bone is a very slow process. The frontal sinus infact remains as a small blind sac within the frontal bone till the child is about 2 years of age, then secondary pneumatization begins. From the age of 2 till the child becomes 9 years old secondary pneumatization of frontal bone proceeds. When the child reaches the age of 9 years, the development of the frontal sinus has reached completion. Sometimes frontal sinus may be asymmetrical or aplastic as well.

The ethmoid sinuses are well-delineated, fluid-filled structures in a newborn child. During fetal development the anterior cells form first, followed by the posterior cells. The cells grow gradually and are adult size by age 12 years.

They are not usually seen on radiographs until age one. The septa gradually become thin and pneumatization spreads as the child ages.

The sphenoid sinuses are unique in that they do not arise from out pouchings of the nasal cavity. These sinuses arise from within the nasal capsule of the embryonic nose. They remain undeveloped until age three. By age seven the pneumatization has reached the sellaturcica. By age 18 the sinuses have reached full size.

PHYSIOLOGY OF MUCOCILIARY CLEARANCE

The movement of the mucous blanket is referred to as mucociliaryclearance. Inflammatory sinus disease results primarily from interference ofmucociliary clearance due to compromise of the drainage portals (osteomeatalchannels) of the individual sinus cavities[3].

The mucosa of the paranasal sinuses and nasal fossae is made up of aciliated cuboidal epithelium that secretes mucus. The cilia are in constant motionand act in concert to propel the mucus in each sinus toward the sinus ostium andthen, once in the nasal fossae, back toward the pharynx. The pattern of flow isspecific for each sinus and persists even if alternative openings are surgicallycreated in the sinus**.**

In the maxillary sinus, mucous flow is directed centripetally toward theprimary ostium. The mucus is then transported through the infundibulum to thehiatus semilunaris, whence it passes into the middle meatus and ultimately intothe nasopharynx.

In the frontal sinus, the mucus flows into the primary ostium down thefrontal recess and then into the middle meatus, where it joins the flow from theipsilateral maxillary sinus**.**

The posterior ethmoid and sphenoid sinuses clear their mucus into thesphenoethmoidal recess. The flow then enters the superior meatus andsubsequently the nasopharynx.

ANATOMY

THE LATERAL NASAL WALL

The anatomy of the lateral wall of the nasal cavity is quite complex. Most of the anatomic anomalies occur here. Usually, individuals have 3 paired turbinates: superior, middle, and inferior. Occasionally, a fourth turbinate, the supreme turbinate, exists. The space between the turbinates along their lateral margin and the lateral walls of the nasal cavity is referred to as the meatus. The inferior turbinate is attached to the lateral wall of the nasal cavity, and only the nasolacrimal duct drains into the inferior meatus.

Most of the inspired airflow travels through the middle meatus rather than through the inferior.

Functionally, the middle meatus is important because the maxillary sinuses, anterior two thirds of the ethmoid sinuses, and frontal sinuses drain into it. Most anatomic variants occur in middle meatus and turbinate region.

The sphenoid sinuses and posterior third of the ethmoid drain into thesphenoethmoid recess in superior meatus.

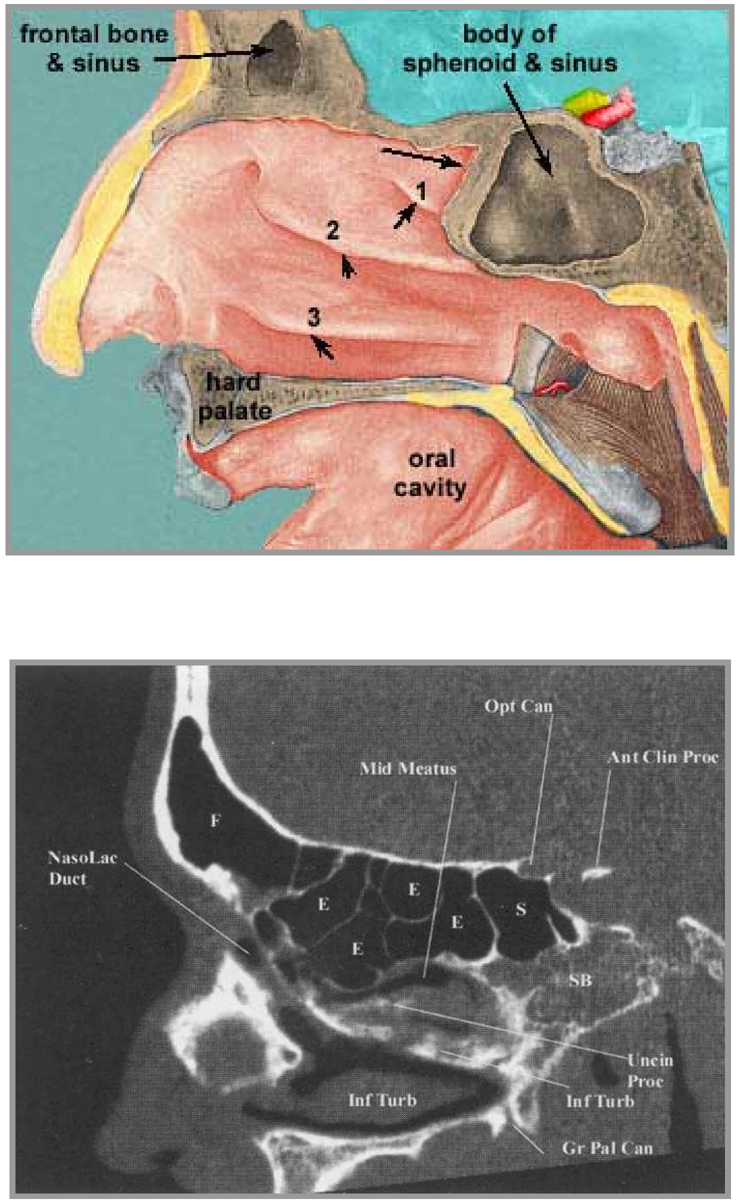

Figure 1: Schematic representation and corresponding sagittal CT image of lateral nasal wall

MAXILLARY SINUSES

The adult maxillary sinus is a pyramid which has a volume of approximately 15 ml.

The base of the pyramid is the nasal wall with the peak pointing toward the zygomatic process. The roof is formed by the orbital floor and transected by the course of the infraorbital nerve.

The posterior wall is unremarkable. Behind this wall is the pterygomaxillary fossa with the internal maxillary artery, sphenopalatine ganglion and the Vidian canal, the greater palatine nerve and the foramen rotundum.

The floor varies in its level. From birth to age nine the floor of the sinus is above that of the nasal cavity. At age nine the floor is generally at the level of the nasal floor. The floor continues to sink as the maxillary sinus pneumatizes.

The natural maxillary ostium is located at the superior aspect of the medial wall of the sinus. The ostium size averages 2.4 mm but can vary from 1 to 17mm. The actual ostium is smaller than that actual bony defect, as mucosa fills this area and defines the extent of the opening. 88% of maxillary ostium are hidden behind the uncinate process and therefore can be visualized only after endoscopic uncinectomy.

Figure 2: Coronal CT image showing maxillary sinuses

UNCINATE PROCESS

The uncinate process is a superior extension of the lateral nasal wall (medial wall of the maxillary sinus)[45].

On CT, the uncinate process can be seen attached inferiorly to the inferior turbinate with the free edge representing the posterior free margin. Anteriorly, the uncinate process may be attached to the lamina papyracea, the skull base or the middle turbinate. This variable superior attachment results in different clinical implications. Laterally this free edge delimits the infundibulum. Posterior to the uncinate process is the ethmoid bulla, usually the largest of the anterior ethmoid cells[6].

Figure 3: Coronal CT image showing the uncinate process

FRONTAL SINUSES

The frontal sinuses have an overall funnel shape, and their aeration varies from patient to patient and from side to side in individual patients.

Some sinuses are small and occupy only the diploic space of the medial frontal bone, while other sinuses can be large enough to extend through the floor of the entire anterior cranial fossa.

In general, a central septation separates the left and right sides; however, often there may be several septations. The floor of the frontal sinus slopes inferiorly toward the midline. Close to the midline, the primary ostium is located in a depression in the floor.

Bent et al. defined frontal cells more specifically as belonging to one of four categories[7].

Type I	Single frontal recess cell above aggernasi cell
Type II	Tier of cells in frontal recess above aggernasi cell
Type III	Single massive cell pneumatizingcephalad into frontal sinus
Type IV	Single isolated cell within the frontal sinus

The frontal sinus opens into the middle meatus medial to the Uncinate process in 88% of the patients and lateral to the uncinate process in 12% of the patients[8].

FRONTAL RECESS

The frontal recess is an hourglass like narrowing between the frontal sinus and the anterior middle meatus through which the frontal sinus drains[4].

It is not a tubular structure, as the term nasofrontal duct might imply, and therefore the term recess is preferred.

The frontal recess usually drains into the middle meatus (62%) or into the ethmoidinfundibilum (38%)[9].

ANTERIOR OSTEOMEATAL UNIT

The anterior OMU includes the frontal sinus ostium, frontal recess,

maxillary sinus ostium, infundibulum, and middle meatus. These channels provide communication between the ipsilateral frontal, anterior ethmoid, and maxillary sinuses.

The gap between the ethmoid bulla and the free edge of the uncinate process defines the hiatus semilunaris.

Medially, the hiatus semilunaris communicates with the middle meatus, the air space lateral to the middle turbinate.

Laterally and inferiorly, the hiatus semilunaris communicates with the infundibulum, the air channel between the uncinate process (caudal border) and the inferomedial margin of the orbit (cranial border).

The infundibulum serves as the primary drainage pathway from the maxillary sinus.

The structure medial to the ethmoid bulla and the uncinate process is the middle turbinate.

Anteriorly it attaches to the medial wall of the aggernasi cell and the superior edge of the uncinate process.

Superiorly it adheres to the lateral edge of the cribriform plate. As it extends posteriorly, the middle turbinate gives a number of posterolaterally coursing bony structures.

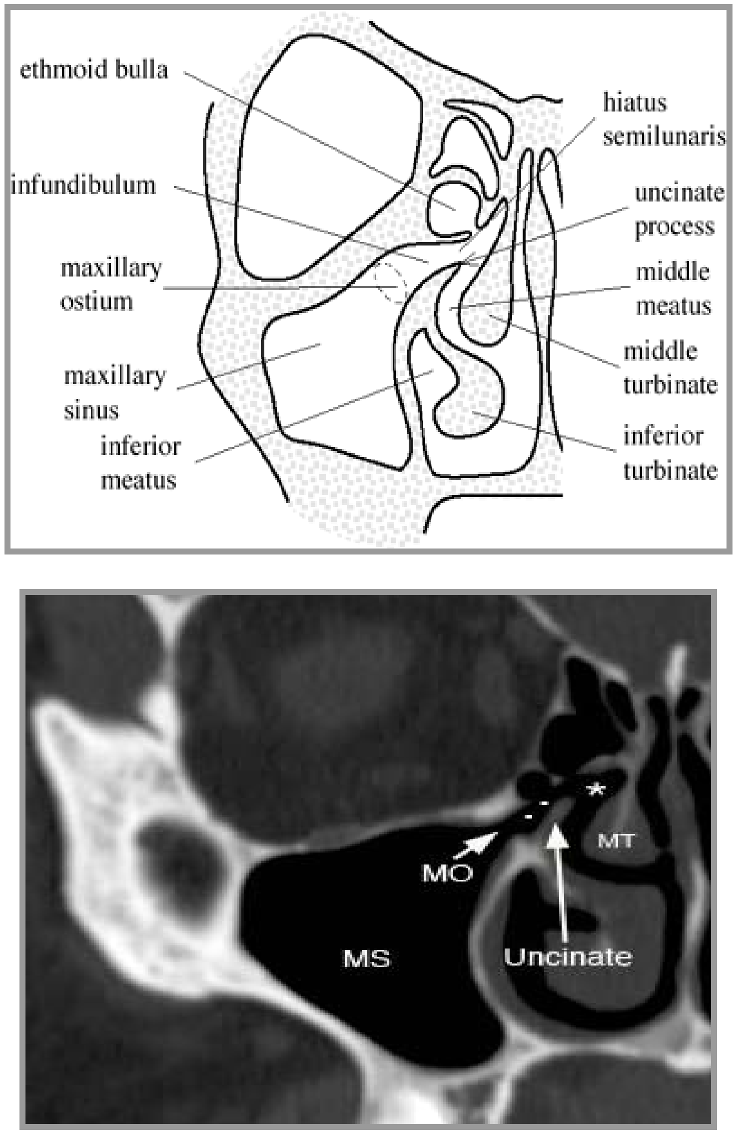

Figure 4: Schematic diagram and coronal CT image of the Osteomeatal unit.

ETHMOIDAL AIR CELLS

Posterior and anterior cells combined have a volume of 15 ml. The ethmoids are shaped like a pyramid and are divided into multiple cells by thin septa. The roof of the ethmoids is composed of multiple important structures. The roof slopes both posteriorly (angle of 15 degrees) and medially.

The anterior 2/3 of the roof is thick and strong and is composed of the frontal bone and the fovea ethmoidalis.

The posterior 1/3 is higher laterally and slopes down medially to the cribriform plate. The junction between the lateral dense bone and the plate is one-tenth as strong as the lateral roof.

The difference in height between the lateral and medial roof is variable, but can be as much as 15-17mm. The posterior aspect of the ethmoid cells borders on the sphenoid sinus.

The lateral wall is the lamina papyracea of the orbit. Among paranasal sinuses, the ethmoid and sphenoid sinuses gain much importance due to their close proximity to the vital structures like orbital contents, cavernous sinus, anterior & middle cranial fossa, optic nerve and internal carotid artery[10].

BASAL LAMELLA (GROUND LAMELLA) OF THE MIDDLE TURBINATE

This structure forms the separation between the anterior and posterior ethmoid cells. It is the attachment of the middle turbinate and runs in three different planes in its course from anterior to posterior.

The anterior most portion is vertical and inserts in the crista ethmoidalis and skull base. The middle third is oblique with insertion in the lamina papyracea. The final third runs horizontal with insertion in the lamina papyracea.

The space under the middle turbinate is termed the middle meatus into which the anterior ethmoids, frontal sinus, and maxillary sinus drain.

Surgical damage to the anterior or posterior portions of the middle turbinate may destabilize this structure and anteriorly risks disruption of the cribriform plate.

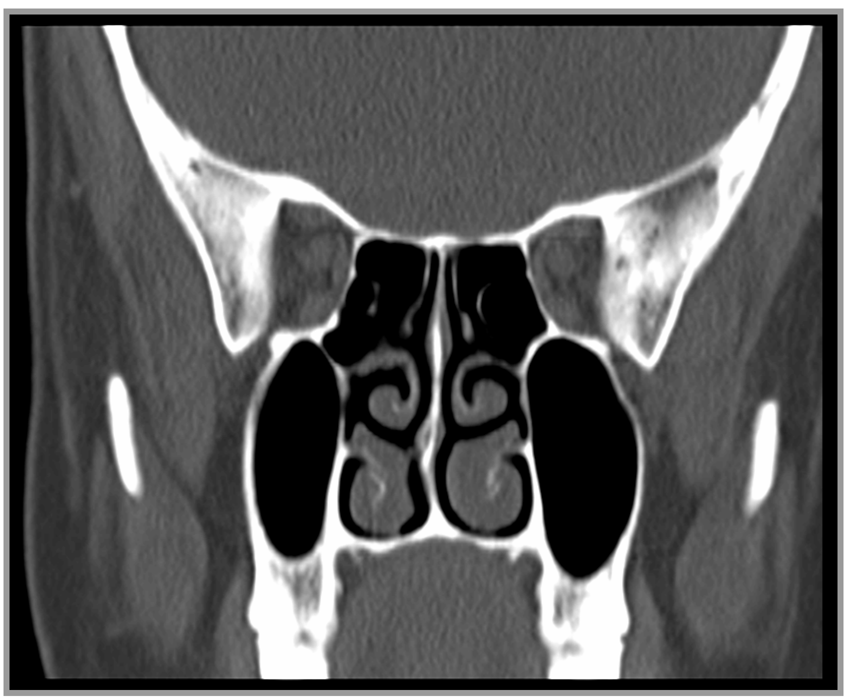

Figure 5: Coronal CT image showing the attachment of middle turbinate.

ANTERIOR Vs POSTERIOR ETHMOID CELLS

The anterior cells are those anterior to the basal lamella. They drain into the middle meatus via the ethmoid infundibulum. The posterior ethmoid sinus consists of air cells between the basal lamella and the sphenoid sinus[6,11,12].

The number, shape and size of these air cells vary significantly from person to person. The posterior cells drain into the superior meatus and border on the sphenoid sinus.

They are generally fewer in number and larger than the anterior cells. Ethmomaxillary Sinus is an enlarged posterior ethmoidal air cell occupying the superior portion of the maxillary sinus draining into superior meatus[13].

ETHMOID INFUNDIBULUM

The development of the infundibulum precedes that of the sinuses. This recess, into which the anterior ethmoid sinuses, maxillary sinus and frontal sinus drain, is formed by multiple structures.

The anterior wall is formed by the uncinate process; the medial wall is the frontal process of the maxilla and the lamina papyracea. It runs anteriorly in continuity with the frontal recess to its posterior limit where the uncinate process attaches to the lamina.

At its anterior end, the ethmoid infundibulum ends blindly in an acute angle, giving rise to the V-like shape noted in axial sections on CT scans[14].

The opening above the recess is known as the hiatus semilunaris. The maxillary sinus drains into this area.

ROOF OF ETHMOID

The roof of the ethmoid is formed by the fovea ethmoidalis of the frontal bone laterally and the cribriform plate of the ethmoid bone medially.

The ethmoid roof is of critical importance for two reasons: Firstly, the bone is thin rendering this area vulnerable to cerebrospinal fluid leaks when breached. Due to the delicate attachment of the middle turbinate to the cribriform plate anteriorly, surgery in this area should be performed with care as detachment of the middle turbinate may damage the dura, resulting in cerebrospinal fluid leak[9].Secondly, the anterior ethmoidal artery is vulnerable to injury which maycause catastrophic bleeding into the orbit.

ETHMOID BULLA

This is the most constant landmark for surgery. It lies above the infundibulum and its lateral/inferior surface and the superior edge of the uncinate process forms the hiatus semilunaris.

It is usually the largest of the anterior ethmoid cells. The anterior ethmoid artery usually courses across the roof of this cell.

Suprabullar and retrobullar recesses may be formed when the ethmoid bulla does not extend to the skull base. The suprabullar recess is a cleft between the roof of the ethmoid bulla and the fovea. The retrobullar space is a cleft between the basal lamella and bulla. This retrobullar space opens into what is known as the "hiatus semilunaris superior**.**

SPHENOID SINUS

The sphenoid sinus is the most posterior sinus. It is usually embedded in the clivus and is bordered superoposteriorly by the sellaturcica. Its ostium is located medially in the anterosuperior portion of the anterior sinus wall and communicates with the sphenoethmoidal recess and the posterior aspect of the superior meatus.

The relationship between the aerated portion of the sphenoid sinus and the posterior ethmoid sinus must be accurately demonstrated. Usually in the paramedian sagittal plane, the sphenoid sinus is the most superior and posterior air space. Horizontally oriented structures within the sphenoid sinus are actually separations between the posterior ethmoid sinuses.

All sphenoid sinus septations are vertically oriented. This relationship is well demonstrated on axial and sagittal images[6,8].

SPHENOETHMOIDAL RECESS

The sphenoethmoid recess is a space behind and above the most superior turbinate. The anterior wall of the sphenoid sinus forms the posterior aspect.

The nasal septum and cribiform plate form the medial and superior aspects.

The anterolateral extent is determined by the most superior turbinate. The space opens into the nasal cavity inferiorly. The posterior ethmoid cells, as well as the sphenoid sinus empty into this region.

The posterior OMU consists of the sphenoid sinus ostium, the sphenoethmoidal recess, and the superior meatus.

RADIOGRAPHIC APPEARANCES OF INFLAMMATORY SINUS DISEASE

ACUTE SINUSITIS:

Acute sinusitis usually is due to bacterial infection of an obstructed paranasal sinus. The obstruction is often the result of apposition of edematous mucosal surfaces from an antecedent viral upper respiratory tract infection.

Acute sinusitis usually involves only a single sinus, with the ethmoid sinus being the most common location[15]. CT features of acute sinusitis include fluid level within the sinus and mucosal thickening.

CHRONIC SINUSITIS:

Chronic sinusitis is diagnosed when the patient has repeated bouts of acute infection or persistent inflammation. The radiographic findings are quite variable. The sinuses most commonly involved with chronic sinusitis are the anterior ethmoid air cells. Certain anatomic variants have been implicated as causative factors in the presence of chronic inflammatory disease.

Opacification of the OMU has been found to predispose patients to the development of sinusitis. Opacification of the OMU without frontal, maxillary, or anterior ethmoid sinus inflammatory disease is rare.

Babbel et al. reviewed 500 patients with screening sinus CT scans and defined five recurring patterns of inflammatory sinonasal disease. The five anatomic patterns were infundibular, OMU, sphenoethmoidal recess, sinonasal polyposis and sporadic or unclassifiable. The infundibular pattern (26% of patients) referred to focal obstruction within the maxillary sinus ostium and ethmoid infundibulum, which was associated with maxillary sinus disease. The OMU pattern (25% of patients) referred to ipsilateral maxillary, frontal and anterior ethmoid sinus disease. This pattern was due to obstruction of the middle meatus. Sparing of the frontal sinus was sometimes seen as a result of the variable location of the nasofrontal duct insertion in the middle meatus.

The sphenoethmoidal recess pattern (6% of patients) resulted in sphenoid or posterior ethmoid sinus inflammation caused by sphenoethmoidal recess obstruction. The sinonasal polyposis pattern (10% of patients) was due to diffuse nasal and paranasal sinus polyps. Associated radiographic findings included infundibular enlargement, convexity (bulging) of the ethmoid sinus walls, and thinning of the bony nasal septum and ethmoid trabeculae[16].

FUNGAL SINUSITIS:

Fungal sinusitis may be suspected clinically when the patient fails to respond to standard antibiotic therapy. Soft tissue changes in the sinus associated with thickened, reactive bone with localized areas of osteomyelitis, and the association of inflammatory sinus disease with involvement of the adjacent nasal fossa and the soft tissue of the cheek should arise high suspicion of fungal sinusitis. These signs of aggressive infection are atypical of bacterial pathogens.

ALLERGIC SINUSITIS:

Allergic sinusitis occurs in 10% of the population and typically produces a pansinusitis with symmetric involvement. CT often shows a nodular mucosal thickening with thickened turbinates. Air fluid levels are rare unless bacterial superinfection occurs.

ORBITAL COMPLICATION OF SINUSITIS:

Patients with sinusitis can develop some form of orbital involvement as complication. These complications are more common in children than in adults, and the orbital manifestation may be the initial clinical signs of sinus infection.

The origin of the infection most commonly is in the ethmoid sinuses. In decreasing order of frequency, the sources of the infection are the frontal, sphenoid, and maxillary sinuses.

HISTORICAL BACKGROUND

CT IMAGING[17]:

Medical imaging has experienced significant changes in both the technologic and clinical areas since the discovery of X-ray in **1895 by Wilhelm Conrad Roentgen,** a German Physicist. Innovations have become common in the Radiology Department, and today the introduction of new ideas and methods and refinements in existing techniques are apparent. One such evolution is the invention of computed tomography (CT).

The first clinical results were presented in 1967 and it became available as practical tool in 1971.

Sir Godfrey Hounsfield, an electronic engineer working at the Central Research Laboratories of EMI in England commenced work on image reconstruction in 1968.His original apparatus consisted of a collimated isotope source mounted on a lathe bed. The objects examined were phantoms contained within a ten-inch water. The scan took 9 days to complete because of the low intensity of the X-ray radiation source, and a further 21/2 hours to process the reading through a computer. The resulting image though of poor quality proved that the system worked. To provide sufficient intensity the equipment was modified by replacing the isotope with an industrial X-ray tube.

A prototype scanner was then developed and installed in Atkinson Morley Hospital in Wimbledon, England on 1st October 1971. The first patient scan was a 41 year old female with suspected frontal lobe tumor, the tumor was clearly demonstrated on the scan.

Cranial pneumography, which is now a thing of the past was introduced by American Neurosurgeon Walter Dandy.Ventriculography (1918) and Encephalography (1919) remained the most effective methods of investigating cerebral tumors and studying the ventricular anatomy for over 40 years. Even after 1950, when cerebral arteriography was introduced, pneumography retained considerable importance and it was not until the introduction of CT in 1973 that its importance began to wane.

Hounsfield and Ambrose presented their paper on CT to the annual congress of the British Institute of Radiology on 20th April 1972 to great acclaim. The first CT papers, by these authors appeared in BJR in 1973. The invention of this technique resulted in the award of 1979 Nobel prize in physiology and medicine to Sir G.N.Hounsfield, Central Research Lab., England (EMI), A.N.Cormack of Physics Department, Tufts University, Massachusetts, U.S.A. Advanced Technological Developments.Over the last ten years , four different generations of CT scan equipment were produced.The most important improvements have been in the reduction in the single image generation time from five minutes to 2.5 seconds in the third and fourth generations scanners and an increase in spatial resolution and contrast.

In the mid-1980s, another high speed CT scanner was introduced, which is referred as the Electron Beam CT (EBCT) scanner used for imaging cardiovascular system. **In 1989, Dr. Willi Kalender** introduced volume scanning by using Spiral / Helical CT scanners. In Spiral/Helical CT Scanners, a thin X-ray beam traces a path around the patient and scans a volume of the tissue.Recently,Dual slice spiral /helical CT scanner and multislice CT scanners were introduced which mainly increase the speed and volume of scan. Volume CT scanning has resulted in a wide range of applications such as CT Fluoroscopy, CT Angiography, Three Dimensional Imaging and Virtual Reality Imaging.

RADIATION DOSE MEASURES: GENERAL DEFINITIONS

Exposure[18]:

The term exposure describes the ability of x-rays to ionize air.

It is measured in roentgens (R); this unit is defined as the quantity of x rays that produces 2.580 x10^{-4} C of charge collected per unit mass (kilograms) of air at standard temperature and pressure (STP): 1 R = 0.000258 C/kg air.

This term refers to the concentration, in air, of radiation at a specific point and is the ionization produced in a specific volume of air. It is typically measured with an ionization chamber and an electrometer.

It essentially describes how much ionization is present in the volume, but it does not tell how much energy is absorbed by the tissues being irradiated.

Absorbed Radiation Dose[18]:

Absorbed radiation dose, often referred to as radiation dose, describes the amount of energy absorbed per unit mass at a specific point. It is measured in grays (1 Gy = 1 J/kg) or rads (1 rad = 100 erg/g). The conversion between rads and grays is 100 rad = 1 Gy.

Absorbed dose essentially describes how much energy from ionizing radiation has been absorbed in a small volume centered at a point; it does not describe where that radiation dose is absorbed or reflect the relative radiosensitivity or risk of detriment to those tissues being irradiated.

Effective Dose[18]:

Effective dose (formerly referred to as the effective dose equivalent) takes into account where the radiation dose is being absorbed (eg, which tissue has absorbed that radiation dose) and attempts to reflect the equivalent whole-body dose that results in a stochastic risk that is equivalent to the stochastic risk from the actual absorbed dose to those tissues irradiated in a nonuniform, partial-body irradiation such as a CT scan.

Effective dose is measured in sieverts (Sv) or rems. The conversion between sieverts and rems is 100 rem = 1 Sv.

RADIATION DOSE OPTIMIZATION

Regardless of model, all CT scanners have a gantry, an x-ray source, and detectors. On passage through the body part, the incident beam is attenuated in a manner dependent on the local tissue composition (greater attenuation for bones, lesser for soft tissues).

FACTORS THAT INFLUENCE RADIATION DOSE FROM CT

In general, there are some factors that have a direct influence on radiation dose, such as the x-ray beam energy (kilovolt peak), tube current (in milliamperes), rotation or exposure time, section thickness, object thickness or attenuation, pitch and/or spacing, dose reduction techniques such as tube current variation or modulation, and distance from the x-ray tube to isocenter.

Beam Energy

Tube potential (peak voltage) determines the incident x-ray beam energy, and variation in tube potential causes a substantial change in CT radiation dose.

The effect of tube voltage on image quality is more complex, since it affects both image noise and tissue contrast.

An important outcome that may be associated with decreased tube voltage is a notable increase in image noise. This occurs if the patient is too large or the tube current is not appropriately increased to compensate for the lower tube voltage.

The dose change is approximately proportional to the square of the tube voltage change (i.e, square of the ratio of final and initial peak voltage), and the noise change is approximately inversely proportional to the tube voltage change[19].

Tube current

Reduction in tube current is the most practical means of reducing CT radiation dose. A 50% reduction in tube current reduces radiation dose by half. The beam energy and photon fluence of an x-ray beam varies with the tube potential and the current used during the particular examination.

Tube current–time product settings are proportional to the number of photons in the defined exposure time (photon fluence).

The radiation dose is directly proportional to the milliampere-seconds value. When all other technical parameters are kept constant, the effective dose values increase linearly with milliampere-seconds.

Any decrease in tube current should be considered carefully, because such reduction causes an increase in image noise, which may affect the diagnostic outcome of the examination. This is especially true in abdominal studies, where low-contrast areas are severely affected by an increase in image noise[19].

Collimation, Table Speed, and Pitch

For helical CT scanners, pitch is defined as the ratio of table feed per gantry rotation to the nominal width of the x-ray beam. An increase in the pitch decreases the duration of radiation exposure to the anatomic part being scanned.

With helical CT scanners, beam collimation, table speed, and pitch are interlinked parameters that affect the diagnostic quality of an imaging study.

Faster table speed for a given collimation, resulting in higher pitch, is associated with a reduced radiation dose (especially if other scanning parameters, including tube current, are held constant) because of a shorter exposure time, whereas narrow collimation with slow table speed, resulting in a longer exposure time, is associated with a higher radiation dose. This is not true for scanners that use an effective milliampere-second setting (defined as milliampere seconds divided by pitch) and maintain a constant value for effective milliampere seconds.

In such scanners, the effective milliampere-second level is held constant irrespective of pitch value, so that radiation dose does not vary as pitch is changed.

For a given collimation, an increase in table speed increases the pitch and reduces the radiation dose by 1 divided by the pitch[20].

Modern multi–detector row scanners may automatically recommend the appropriate tube current adjustment to maintain a given image noise level when pitch is changed.

Although scanning at a higher pitch is generally more dose efficient, it also tends to cause helical artifacts, degradation of the section-sensitivity profile (section broadening), and decrease in spatial resolution. Hence, alterations in pitch can have varying effects on image quality in different situations.

Scanning Modes

Use of a multi–detector row CT scanner results in some amount of unused radiation extending beyond the beginning and end of the imaging region[21].

This occurs because, at the start of the acquisition, only the first detector row is contributing to the image. As the acquisition proceeds, additional detector rows enter the imaging region until all rows are contributing. A similar effect occurs in reverse at the end of the acquisition.

As a result, it is generally more dose efficient to use a single helical scan rather than multiple helical scans if there are no overriding clinical considerations, such as breath holding, for the patient. The need to prescribe multiple contiguous helical scans should be infrequent with modern high-speed multi–detector row scanners.

Gantry Rotation Time

There has been a dramatic decrease in tube rotation times with recent technologic innovations, most notably with the development of four–, eight–, and 16–detector row CT scanners.

Whereas a four-row scanner with a 0.8- second rotation time requires a 16-second breath hold to scan the entire abdomen, an eight-row scanner covers this length in 8 seconds.

If the tube rotation time is decreased (faster gantry rotation), the radiation exposure decreases, and tube current may thus have to be increased to maintain constant image quality[19].

Modern 16-row scanners are capable of high scanning speeds and submillimeter section thicknesses. Thin collimation can lead to a higher dose, especially if tube current is increased to maintain image noise at a level similar to that of thicker sections. The contrast resolution of small lesions improves because of reduced partial volume effects; hence, greater noise on thinner sections may often be acceptable[22].

In addition, submillimeter- collimation scans can usually be reconstructed as thicker sections, which reduce inherent noise. Thus, it is important to optimize beam collimation for different multi–detector row scanners on the basis of the clinical situation in question.

Radiation protection:

The triad of radiation protection actions comprise of "time-distance-shielding". Reduction of exposure time, increasing distance from source, and shielding of patients and occupational workers have proven to be of great importance in protecting patients, personnel, and members of the public from the potential risks of radiation.

It has been recommended that the thyroid, breast and gonads of the patients be shielded, to protect these organs especially in children and young adults. In gonadal shielding, a lead apron is placed appropriately on the patient to protect the gonads from primary beam radiation exposure. A lead bib and collar worn over the patient's neck and thorax have been documented to effectively shield radiosensitive organs like the thyroid and the breast, and are therefore recommended for routine use in head CT examinations.

ESTIMATING EFFECTIVE DOSE FROM CT

The definition of effective dose was given earlier [23] as the weighted sum of organ doses resulting from the examination, where the radiosensitive organs were defined along with their tissue-weighting factors. Although it appears straightforward to estimate effective dose, it is actually difficult to accurately estimate the dose to an individual organ from a CT scan. This is even more difficult when attempting to estimate the effective dose for each patient when each one has unique characteristics of height, weight, age, gender, and composition. Many methods are in practice for calculating the effective dose.

One of the widely used methods to estimate the effective dose involves conversion factors for a general anatomic region as described by the European Guidelines on Quality Criteria for Computed Tomography[24], which are based on the work of Jessen et al[25].

In this approach, the CTDIvol and distance are used to estimate the DLP, which is then multiplied by a region-specific conversion factor to estimate the effective dose. These conversion factors range from 0.0023 mSv/mGy x cm for the head region to 0.017 mSv/ mGy x cm for the chest region and 0.019 mSv/ mGy x cm for the pelvis. This approach obviously does not take into account any patient-specific or even examination-specific factors but provides an easily estimated value of effective dose.

REVIEW OF LITERATURE

Computerized tomography (CT) is the gold standard for visualization of anatomy of paranasal sinuses and to determine the extent of disease, both of which are important for endoscopic sinus surgery. CT helps in providing important structural landmarks, which are critical to help avoid complications such as absent uncinate process or asymmetry of cribriform niche. Although MRI is also being increasing employed for evaluation of sinusitis, it is limited in providing information on bony anatomy with increased risk of potential over-diagnosis. It was concluded that while MRI may be a great choice for differentiating neoplastic disease, it has only limited role in evaluation of sinusitis[26].

Imaging of paranasal sinuses has undergone tremondous change with the availability of CT scans. The anatomy of paranasal sinuses can be visualised with greater details, which was not available before. This has made the radiologist a key member of the patient management team[27].

With the introduction of functional endoscopic sinus surgery (FESS), radiographs are seldom used as part of diagnostic work-up in a patient with sinusitis. CT is considered the standard test for evaluation of sinusitis. However, CT evaluation of paranasal sinuses is associated with increased risk of radiation to important structures such as lens and thyroid gland, which may result in complications such as cataract of eye[28].

Patient radiation exposure during CT is related to the choice of tube current setting, tube voltage, section thickness, pitch, and gantry cycle time. Reduction in tube current is the most practical means of reducing CT radiation dose. A 50% reduction in tube current reduces radiation dose by half. Although reduction tube current or tube voltage results in decrease in radiation exposure it is also associated with an increase in image noise, which may compromise the diagnostic quality of the obtained images. Therefore, although it is crucial that radiation dose be reduced, it should not impact the diagnostic quality of images[29].

A study was conducted by **Sohaib et al,**to evaluate the effect of reduction of tube current on diagnostic quality of images and the radiation dose received by orbit (lens in particular)in individuals who underwent CT of paranasal sinuses. Patients were assigned to different groups with radiation dose progressively reducing from 200 mAs to 50 mAs across different groups. Reduction of the tube current value does not compromise the diagnostic efficacy of the study. A semi-quantitative scoring was used to assess 6 anatomical landmarks with scores of 0, 1 and 2 assigned to structure not demonstrated, demonstrated but not clearly visualized and clearly demonstrated respectively. The results showed no significant difference between standard-dose CT (100-200 mAs) and low-dose CT (50 mAs) with regards to image quality based on the scoring system. Mean radiation dose to orbit was significantly reduced from 13.5 mGy at 200 mAs to 3.1 mGy at 50 mAs (77% reduction). It was concluded from the study that low-dose CT scan should be strongly considered for CT evaluation of sinuses as it reduces radiation dose to the patient without affecting diagnostic quality of study.[30].

Tack et alconducted a study in 50 patients with chronic sinusitis to compare low- and standard-dose multidetector CT (MDCT) findings in patients with suspected chronic sinusitis. Patients underwent CT scans with radiation ranging from 10 to 150 effective mAs. Assessment was performed to evaluate bony and mucosal abnormalities. The authors concluded from the study that dose reduction did not play a significant role in detection of discrepancies as compared to human element of reviewer observation. It was also concluded from the study that low-dose CT should be considered to be method of choice for evaluation of suspected chronic sinusitis as it provided significant reduction in radiation[31].

A study by **Kasim et al** evaluated the reliability of low-dose CT when compared with plain radiography. It was concluded from their study that reliability of low-dose CT is significantly higher than that of plain radiography and equal to that of the standard CT for pediatric age group in the investigation of paranasal sinuses with an effective dose less than routine plain radiograph. There was also significant interobserver and intraobserver agreement with low-dose CT in terms of detection of pathology and pathology characterization.[32].

A study was conducted by **Lam et al**in 30 patients to compare image quality of paranasal sinuses with low-dose (40 mAs) and standard-dose (100 mAs) CT protocol based on a subjective assessment scoring and to determine potential radiation dose reduction to thyroid gland and eyes. The results did not show any significant difference in the assessment scores between both the groups in terms of image quality. Additionally there was significant reduction in radiation received by eye and thyroid gland with low-dose CT scan. The authors recommended use of low-dose CT technique for evaluation of paranasal sinuses[33].

Hojreh et al conducted a study to define objective and reproducible standards for quality of CT images with different radiation doses and their therapeutic validity. The pixel noise has been shown to be indicative of image quality of pasanasal sinuses. It was shown from the study that use of low-dose protocols and edge-enhancing reconstruction algorithms can be indicated in CT evaluation of chronic sinusitis. Although there is reduction in pixel noise with high-dose protocols the authors recommend refraining from these techniques[34].

Akaylehconducted a study in 60 patients in patients with suspected sinusitis to compare the quality of CT images with low-dose and standard-dose CT. Standard dose CT was obtained using 451 mAs in axial projection and 503 mAs in coronal projection. Low dose CT was performed using 16 mAs in axial projection and 23 mAs in coronal projection. It was demonstrated that low-dose CT was equally effective to high-dose CT in evaluation of chronic sinusitis in both coronal and axial projections. The author recommended low-dose CT for evaluation of sinusitis[35].

Duvoisin et al conducted a prospective study to evaluate the role of low-dose CT with standard dose-CT in imaging of paranasal sinuses. It was seen in the study that mAs setting of as low as 30 mAs can be used in the evaluation of sinusitis without significant compromise in image quality. Additionally, the disease extent was accurately idenfitied without any false negative results. The authors concluded that low-dose CT should be preferred with few sections obtained with standard dose CT wherever required[36].

Hagtvedt et al conducted a study in 47 patients to compare low-dose CT examination with standard-dose CT and plain film radiograph. All the patients underwent standard-dose Ct, low-dose CT and plain radiography for evaluation of sinusitis. Low-dose CT protocol consisted of 10 coronal scans using 40 mAs and 1 mm collimation. The results showed an overall sensitivity of low-dose CT to be 85% and specificity to be 97% when comapred with standard dose CT. It was concluded from the study that image quality with low-dose CT is comparable to standard-dose CT with low radiation exposure compared to standard-dose CT for evaluation of chronic sinusitis and should be considered the method of choice in patients referred for sinusitis[37].

Hagtvedt et al compared the efficacy of detection of sinusitis with low-dose and standard-dose CT in patients with suspected acute sinusitis. Compared to standard-dose CT, low-dose CT showed high specificity of >96% for all sinus groups and high sensitivity of >95% execpt for frontal sinus, which had a sensitivity of 83%. It was concluded from the study that low-dose CT offers significant dose reduction and can be considered the standard of imaging in patients with suspected acute inflammatory paranasal disease[38].

Bulla et al conducted a study in 80 patients who underwent CT of paranasal sinuses to evaluate the image quality of dose-reduced CT of paranasal sinus using iterative reconstruction technique. In this study patients underwent CT with standard setting of 60 mAs and reconstructed with filtered back projection and then low dose techniques of 48 mAs, 36 mAs and 24 mAs with image reconstruction using iterative reconstruction technique. The results showed that compared to filtered back projection, iterative reconstruction can help in reducing radiation dose by up to 60% without significantly affecting diagnostic quality of the CT images[39].

MATERIALS AND METHODS

Source of data:

This prospective study was carried out on 60 patients who presented with clinically suspected paranasal sinusitis over a period of 18 months from January 2013 to June 2014 in the department of radio diagnosis of R L Jalappa hospital and research Centre, Tamaka, Kolar.

Inclusion Criteria:

1. All patients with clinically suspected sinusitis or recurrent sinusitis.

Exclusion Criteria:

1. All cases of trauma.
2. Previous history of sinonasal surgery.
3. Patients suspected to have other pathologies of paranasal sinuses.
4. Patients below the age of 18 years.

Method of collection of data:

After an informed consent was taken, alternate patients were taken up for low dose MDCT (130 kV and 40 mAs) and standard dose MDCT (130 kV and 60 mAs) of the paranasal sinuses.

The patients scanned by standard dose protocol were included under group A (Control) and the patients scanned by the low dose protocol were included under group B (Cases).

All the patients in this study were scanned with SIEMENS SOMATOM EMOTION 16 CT scanner.

PARAMETERS USED FOR LOW DOSE SINUS CT

Non-contrast helical scanning was performed using the 16-slice CT scanner (Siemens SOMATOM Emotion 16, Forschheim, Germany) in axial sections covering the region from the top of the frontal sinuses to the hard palate .The scans were acquired in a cranio-caudal order.

The low dose protocol comprised of the following parameters,

- A fixed KVp of 130, slice collimation of 16 x 0.75 mm.
- Slice width of 3.0 mm.
- Feed per rotation of 6.0 mm.
- Rotation time of 0.5.
- Pitch of 0.55.
- Effective mAs of 40.

The scans were reconstructed using Kernel H60f sharp in osteo window and Kernel H30 smooth in soft tissue window. A 512 x 512 image matrix was used. From the volumetric raw data of both scanning protocols, the images of each patient were reconstructed using filtered back projection in 1.0 mm thickness with an increment of 0.75 mm.

For comparison 30 alternate patients were examined with standard CT of the sinuses (130 kV and 60 mAs).

IMAGE QUALITY ASSESSMENT:

Diagnostic image quality is assessed by scoring for six anatomical structures and visualization of pathological processes:

1. Maxillary ostium.
2. Uncinate process.
3. Infundibulum.
4. Frontal recess.
5. Attachments of the middle turbinate.
6. Path of the optic nerve.
7. Pathological process.

For each structure, the following score was allocated depending on how well each was visualized:

- ✓ 0, not demonstrated;
- ✓ 1, demonstrated but not clearly visualized;
- ✓ 2, clearly visualized.

CALCULATION OF EFFECTIVE DOSE:

The dose length product (DLP) was got from the dose report given by the machine at the end of each scan.

Based on the European Guidelines on Quality Criteria for Computed Tomography[24] and works of Jessen et al[25], the effective dose of the scan was calculated by multiplying the dose length product with a factor of 0.0023.

Effective Dose (ED) = DLP x 0.0023 mSv.

RESULTS

Table 1 shows the age distribution of the patients who were included in the study. The age distribution in both low-dose and regular group are similar. Similar trends are seen in gender distribution (table 2).

Table 1: Age distribution of patients studied

Age in years	Low dose Group		Regular Group	
	No	%	No	%
18-20	5	16.7	4	13.3
21-30	11	36.7	9	30.0
31-40	4	13.3	7	23.3
41-50	5	16.7	6	20.0
51-60	2	6.7	2	6.7
61-70	2	6.7	2	6.7
>70	1	3.3	0	0.0
Total	30	100.0	30	100.0
Mean ± SD	**36.30±15.03**		**35.10±13.20**	

Samples are age matched with P=0.744

Graph 1: Age distribution

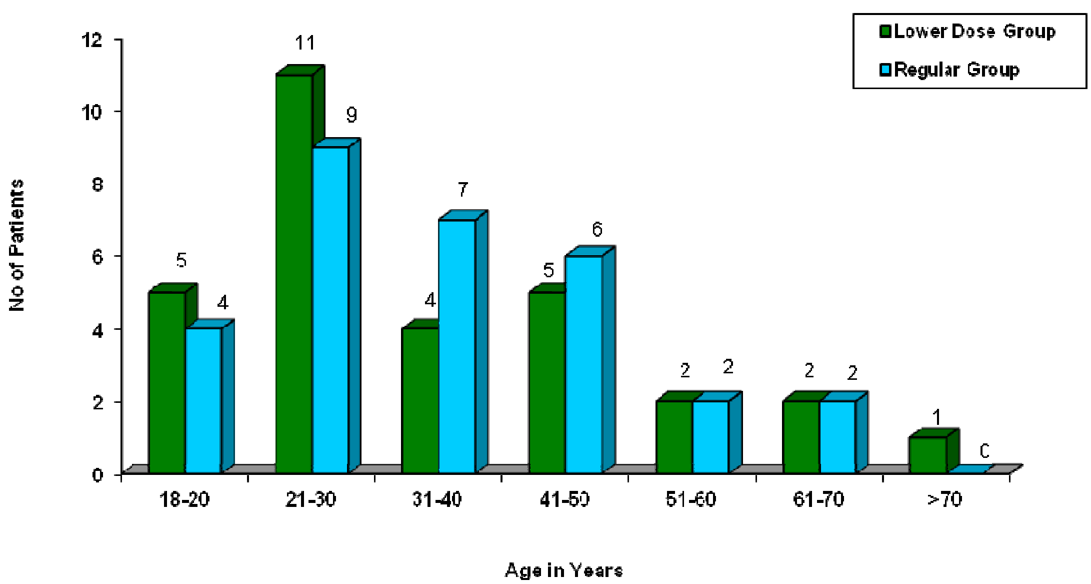

Table 2: Gender distribution of patients studied

Gender	Low dose Group		Regular Group	
	No	%	No	%
Female	16	53.3	12	40.0
Male	14	46.7	18	60.0
Total	**30**	**100.0**	**30**	**100.0**

Samples are gender matched with P=0.301

Graph 2. Gender distribution

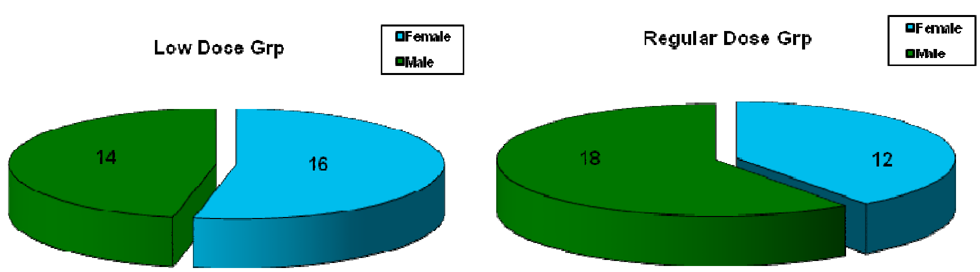

The maxillary sinus was the most common sinus involved across both the study groups followed by ethmoidal sinus (table 3). This shows that maxillary sinus is the commonest sinus involved in sinusitis followed by ethmoidal.

Table 3: Distribution of sinuses involved

Sinus involved	Low dose Group		Regular Group		P value
	No	%	No	%	
Frontal	10	33.3	12	40.0	**0.592**
Ethmoid	17	56.7	20	66.7	**0.426**
Maxillary	26	86.7	26	86.7	**1.000**
Sphenoid	11	36.7	7	23.3	**0.260**

Graph 3: Distribution of sinuses involved

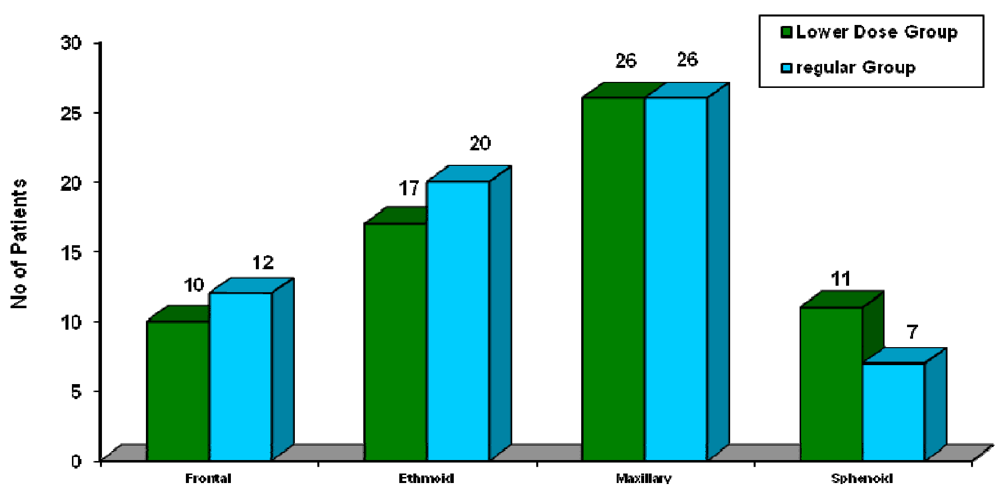

Table 4 shows the results of maxillary ostium assessment with low dose and regular dose protocols. The results are consistent between both the groups.

Table 4: Visualization of maxillary ostium

Maxillary ostium	Low dose Group (n=30)		Regular Group (n=30)	
	No	%	No	%
0	0	0.0	0	0.0
1	0	0.0	0	0.0
2	30	100.0	30	100.0

Graph 4: Visualization ofostium

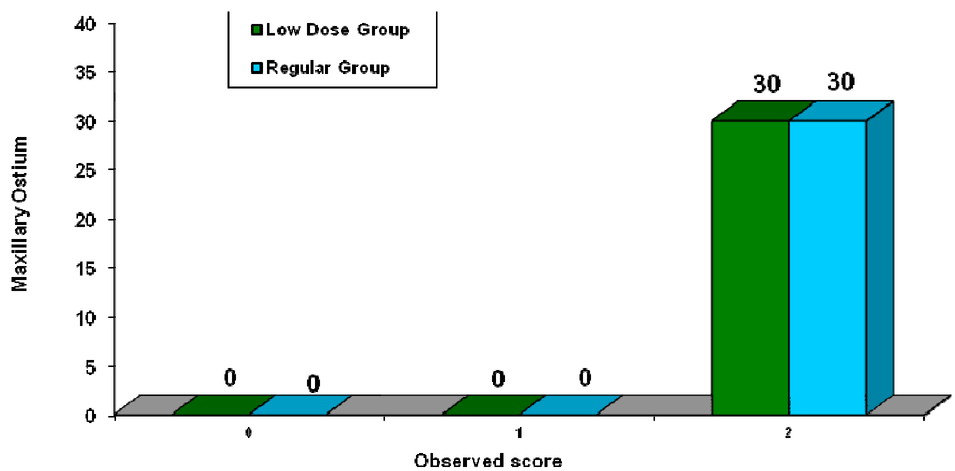

Similarly uncinate process was visualized in all the participants in low dose and regular dose group (table 5).

Table 5: Visualization of uncinate process

Uncinate process	Low dose Group (n=30)		Regular Group (n=30)	
	No	**%**	**No**	**%**
0	0	0.0	0	0.0
1	0	0.0	0	0.0
2	30	100.0	30	100.0

Graph 5: Visualization of uncinate process

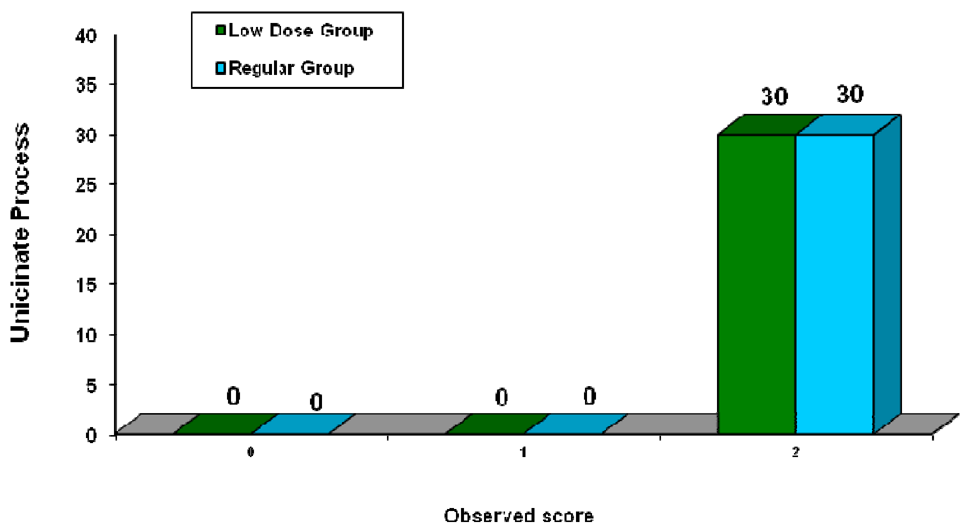

Infundibulum was seen in all the participants involved in low dose and standard dose group. However, in one patient in low dose group it was not clearly demarcated and hence a score was 1 was given; however this was not statistically significant (P=0.492).

Table 6: Visualization of infundibulum

Infundibulum	Low dose Group (n=30)		Regular Group (n=30)		P value
	No	%	No	%	
0	0	0.0	0	0.0	-
1	1	6.7	0	0.0	**0.492**
2	29	96.7	30	100.0	**1.000**

Graph 6: Visualization of infundibulum

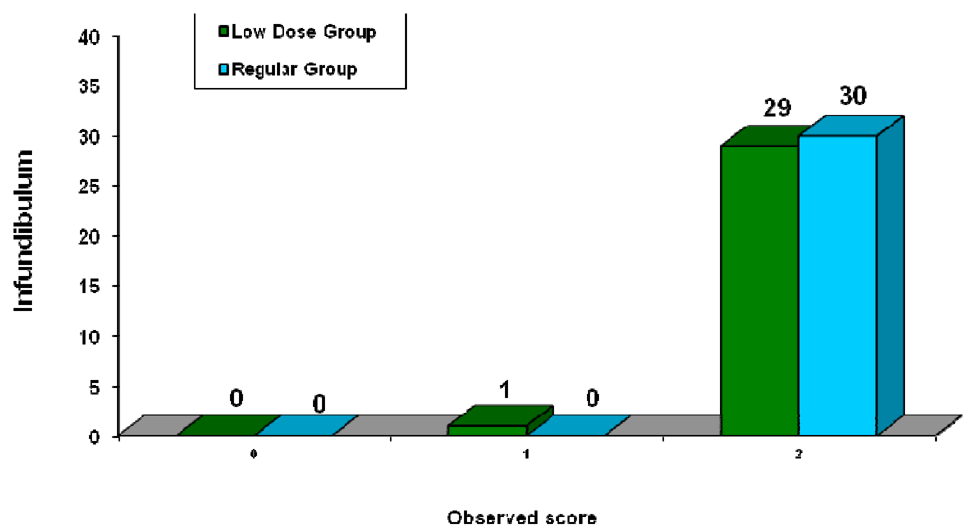

Frontal recess was seen in all participants included in the low-dose and regular dose group (table 7).

Table 7: Visualization of frontal recess

Frontal recess	Low dose Group (n=30)		Regular Group (n=30)	
	No	**%**	**No**	**%**
0	0	0.0	0	0.0
1	0	0.0	0	0.0
2	30	100.0	30	100.0

Graph 7: Visualization of frontal recess

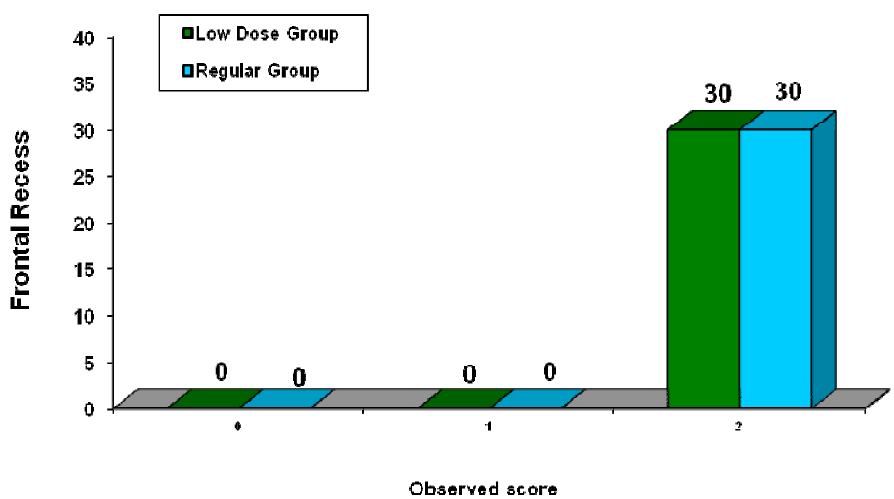

Similar results were also seen for visualization of attachments of middle turbinates across both the groups (30 vs 30 in low-dose and regular-dose group respectively). (Table 8)

Table 8: Visualization of attachments of middle turbinates

Attachments of middle turbinates	Low dose Group (n=30)		Regular Group (n=30)	
	No	%	No	%
0	0	0.0	0	0.0
1	0	0.0	0	0.0
2	30	100.0	30	100.0

Graph 8: Visualization of attachments of middle turbinates

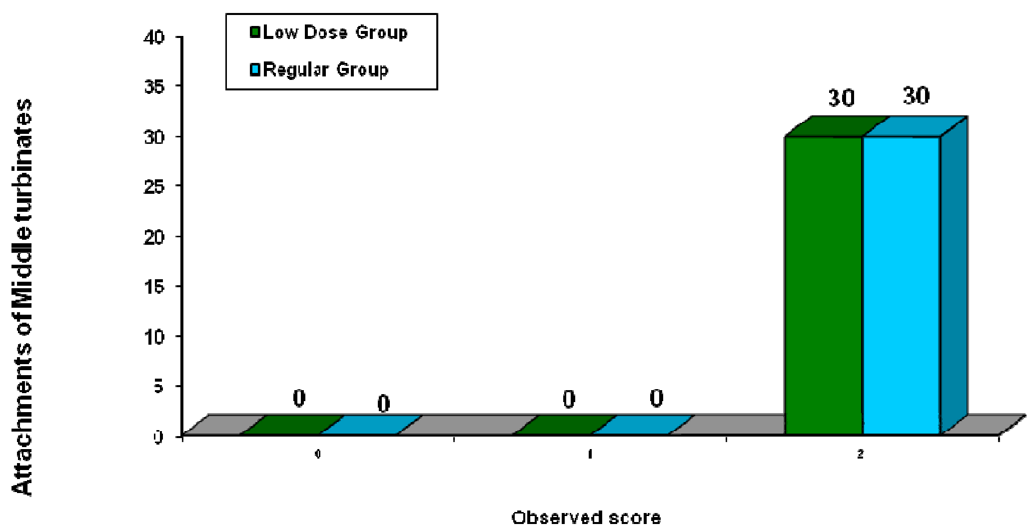

Optic nerve pathway and pathological changes were seen in all participants included in the low-dose and standard dose group (Tables 9 and 10 respectively).

Table 9: Visualization of pathway of optic nerve

Pathway of optic nerve	Low dose Group (n=30)		Regular Group (n=30)	
	No	%	No	%
0	0	0.0	0	0.0
1	0	0.0	0	0.0
2	30	100.0	30	100.0

Graph 9: Visualization of pathway of optic nerve

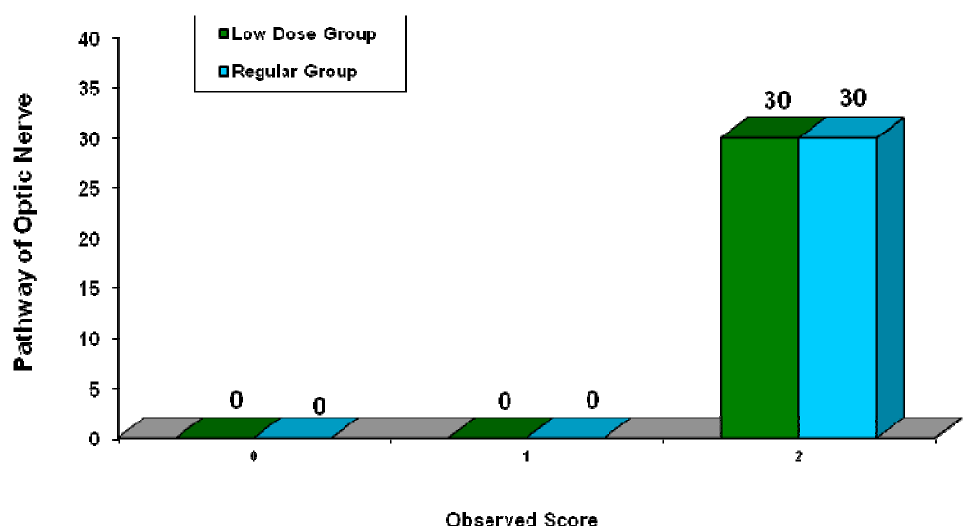

Table 10: Visualization of pathological changes

Pathological changes	Low dose Group (n=30)		Regular Group (n=30)	
	No	**%**	**No**	**%**
0	0	0.0	0	0.0
1	0	0.0	0	0.0
2	30	100.0	30	100.0

Graph 10: Visualization of pathological changes

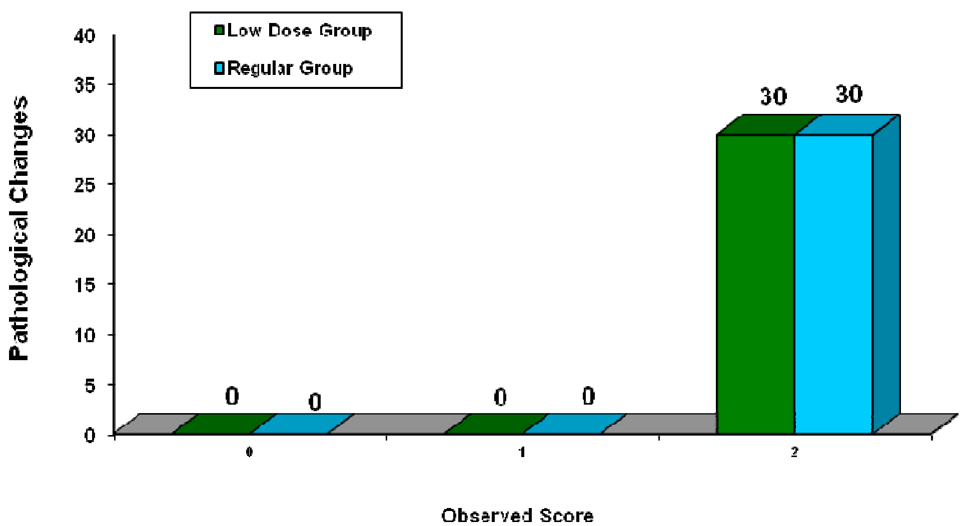

The combined results across all the anatomical structures and pathology are depicted in Table 11. In the low dose group, 29 patients had a score of 14 compared with all patients (n = 30) in the regular dose group. Only one patient had a score of 13, as infundibulum was not clearly demarcated in that participant. However, the difference was not statistically significant (P = 0.492).

Table 11: Total (Max - 14)

Total (Max Score - 14)	**Low dose Group**		**Regular Group**	
	No	**%**	**No**	**%**
13	1	6.7	0	0.0
14	29	93.3	30	100.0
Total	**30**	**100.0**	**30**	**100.0**

P=0.492

Graph 11: Total (Max Score - 14)

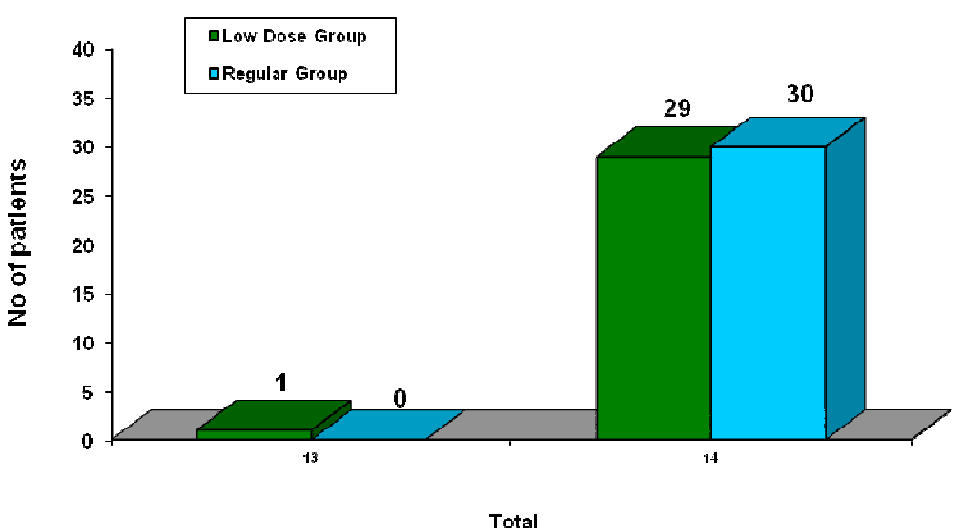

The effective radiation dose received by the patient was <0.36 mSv in all the patients included in the low dose group compared to only one patient in the regular dose group. Remaining 29 participants of regular dose group received effective radiation dose of >0.36 mSv.

Table 12: Effective dose (mSv)

Effective Dose	Low dose Group		Regular Group	
	No	%	No	%
<0.36	30	100	1	3.3
0.36-0.42	0	0	25	83.3
>0.42	0	0	4	13.3
Total	**30**	**100**	**30**	**100.0**

Graph 12: Effective dose (mSv)

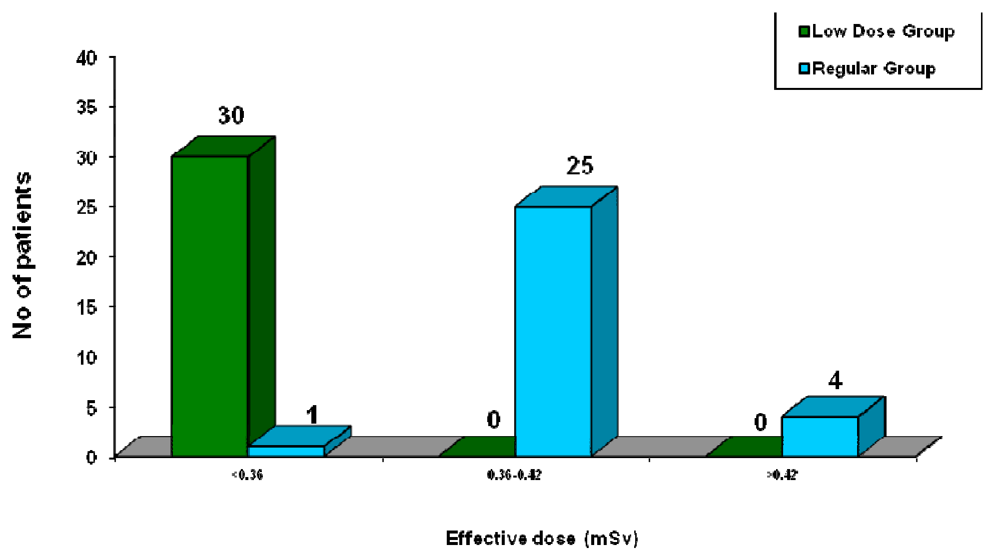

When the mean effective dose was calculated, the mean effective dose in low dose group was 0.26 mSv and 0.38 mSv in regular group, resulting in 31% reduction in radiation with use of low dose CT.

Table 13: Mean effective dose

	Low dose Group	Regular Group
Effective Dose (mSv)	**0.26**	**0.38**

Graph 13: Mean effective dose

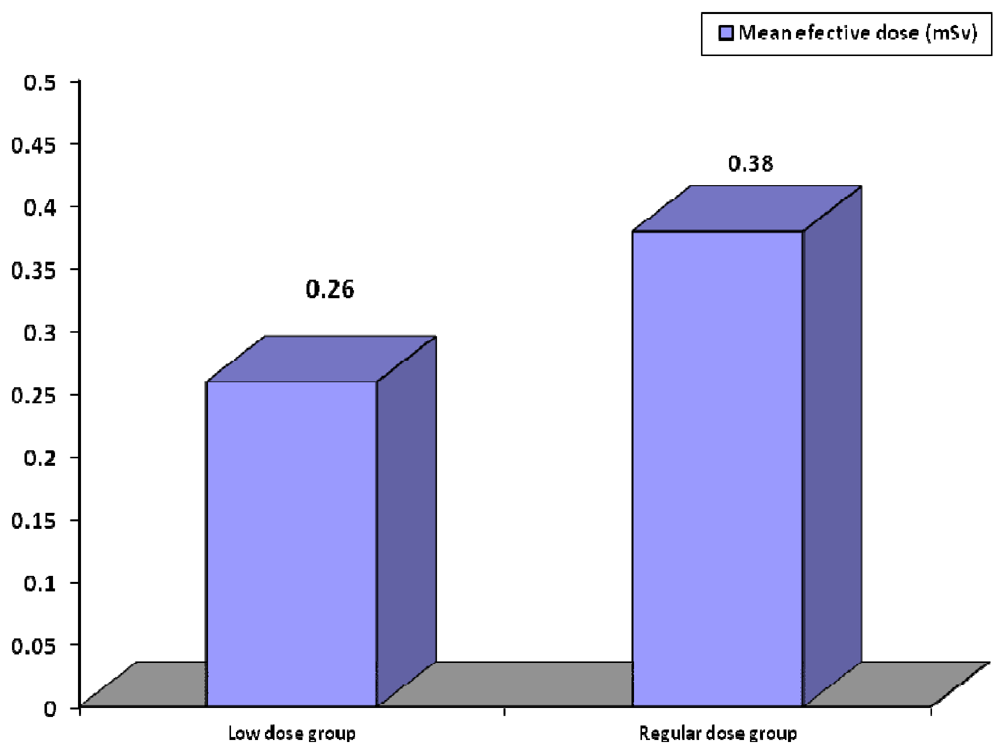

Figure 6 A and B: Coronal images of MDCT scans obtained at 60 mAs (A) and 40 mAs (B) at the level ofthe maxillary sinuses show the uncinated process. No significant difference in the diagnostic image quality of these two scans.

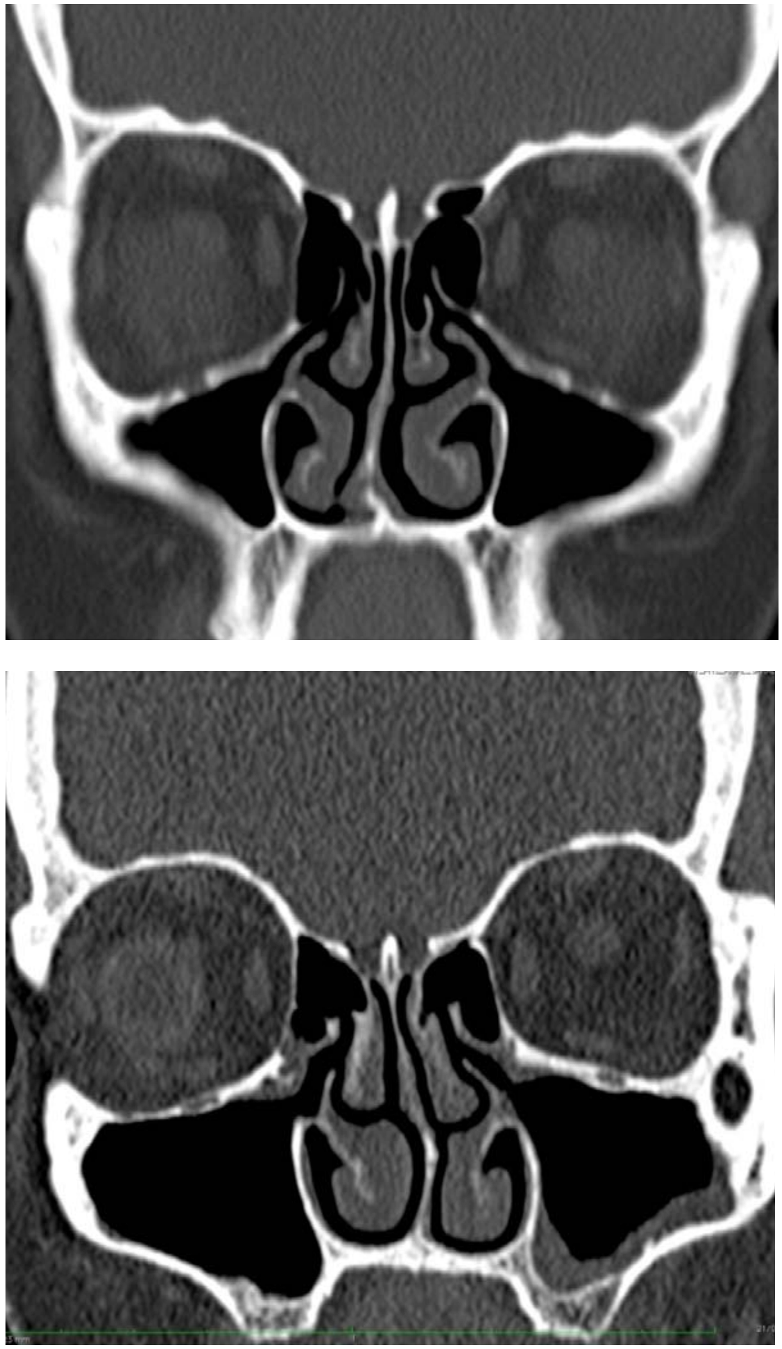

Figure 7 A and B: Coronal images of MDCT scans obtained at 60 mAs (A) and 40 mAs (B) at the level ofthe maxillary sinuses show the maxillary ostium. No significant difference in the diagnostic image quality of these two scans.

Figure 8 A and B: Coronal images of MDCT scans obtained at 60 mAs (A) and 40 mAs (B) at the level ofthe maxillary sinuses show the infundibulum. No significant difference in the diagnostic image quality of these two scans.

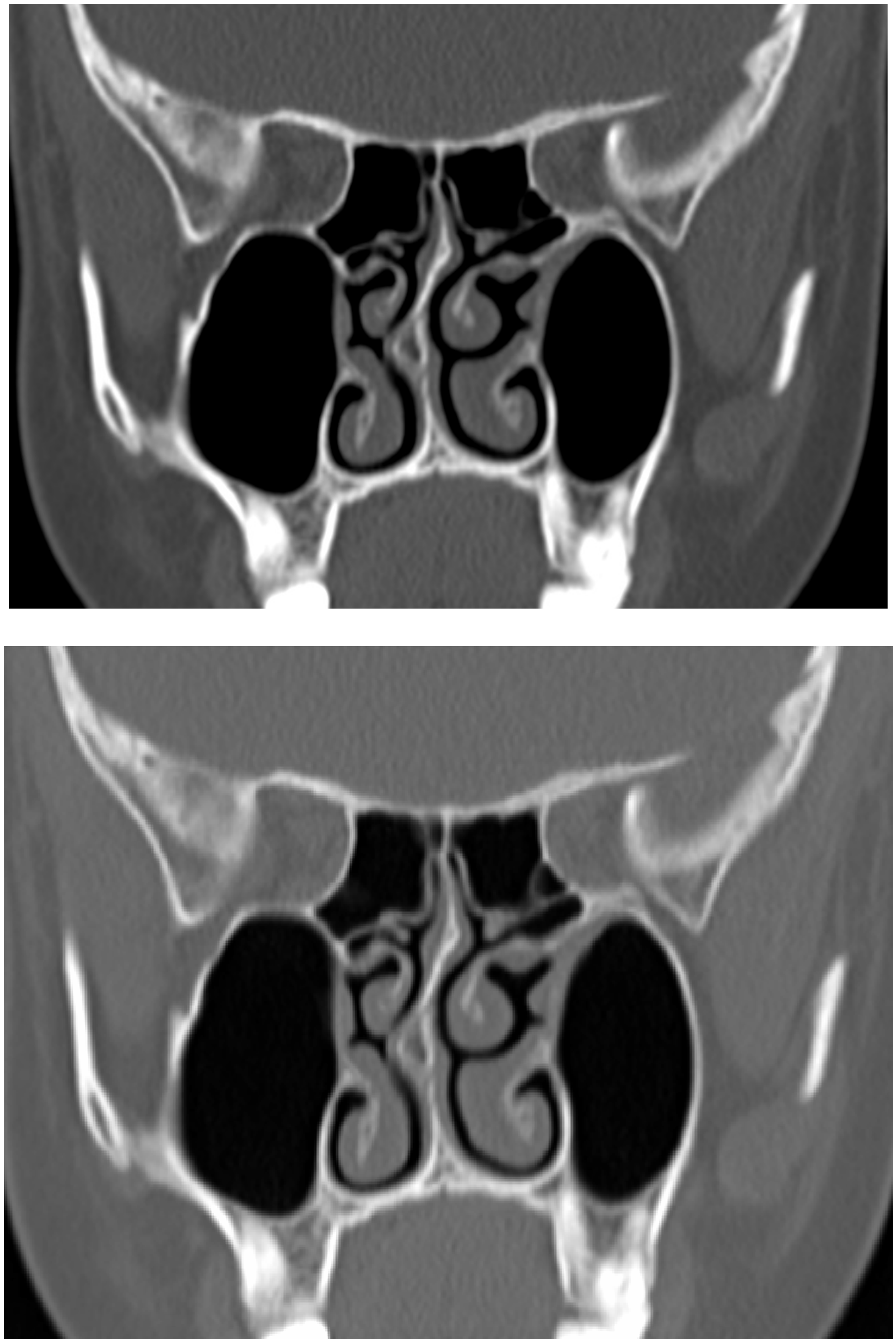

Figure 9 A and B: Coronal reformatted images of MDCT scans obtained at 60.mAs (A) and 40 mAs (B) showing the attachments of middle turbinates. This structure is clearly identified and correctly assessed in both the scans.

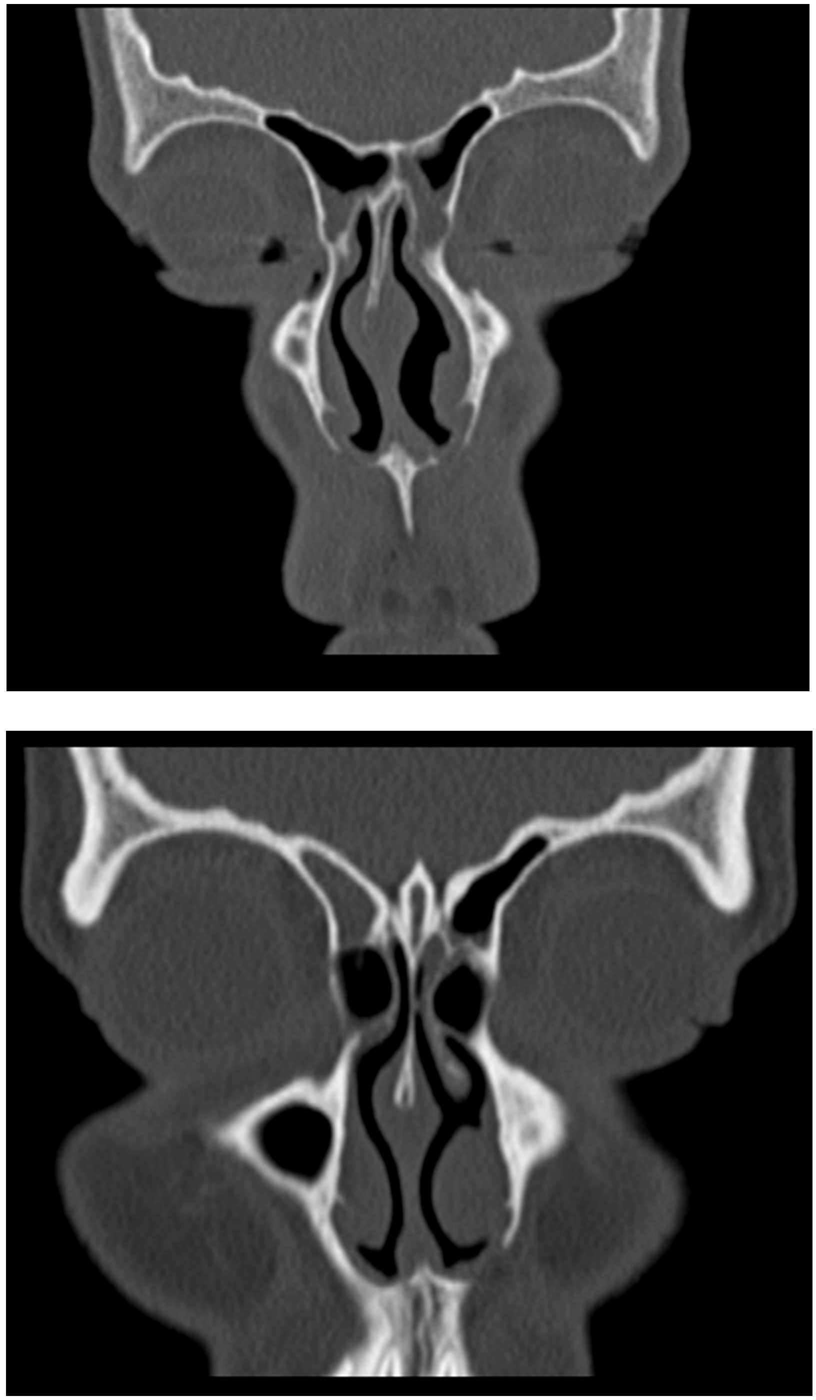

Figure 10 A and B: Coronal reformatted images of MDCT scans obtained at 60.mAs (A) and 40 mAs (B) showing the frontal recess. This structure is clearly identified andcorrectly assessed in both the scans.

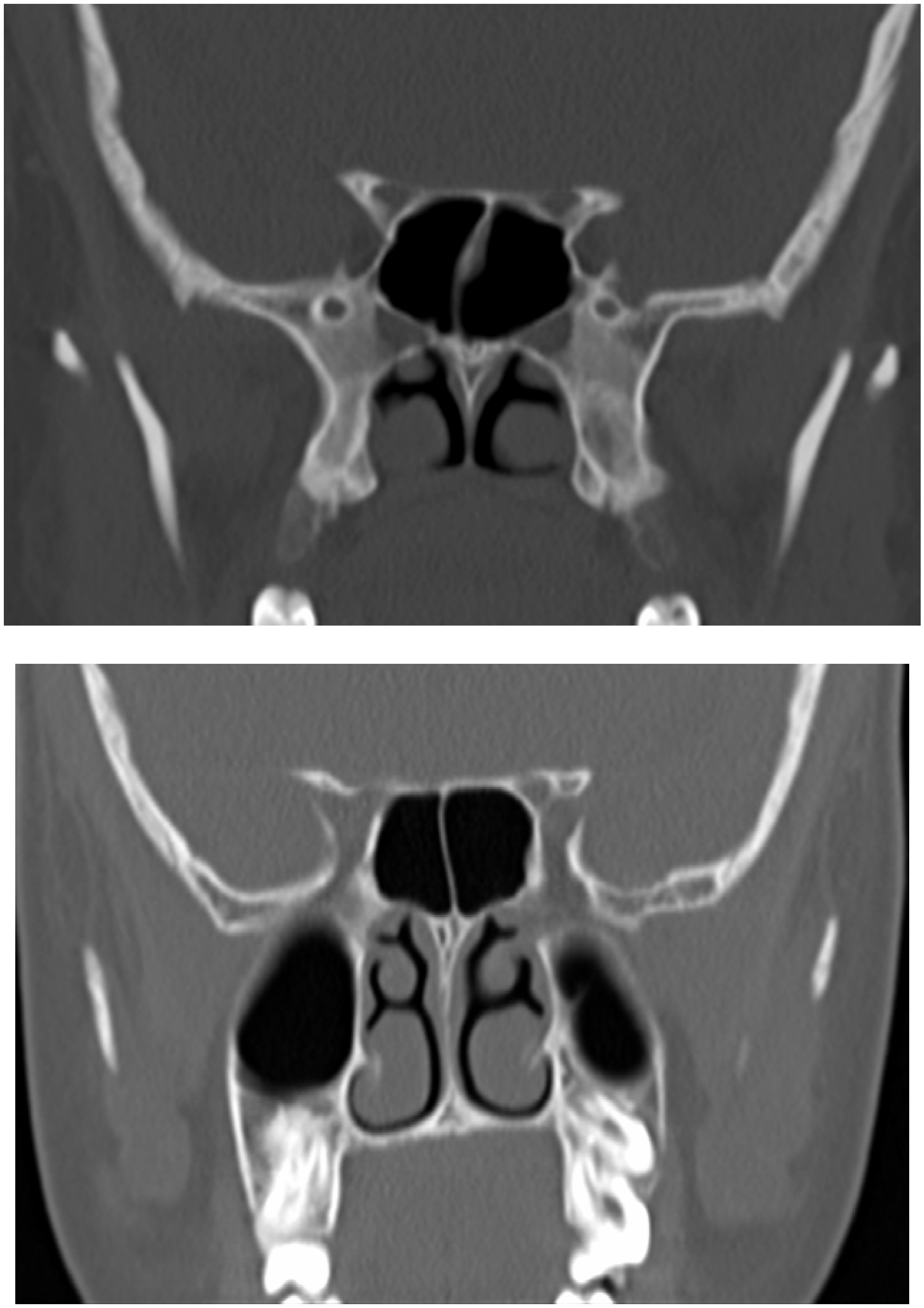

Figure 11 A and B: Coronal reformatted images of MDCT scans obtained at 60.mAs (A) and 40 mAs (B) showing the pathway of optic nerves (arrow). This structure is clearly identified andcorrectly assessed in both the scans.

Figure 12 A and B: Coronal reformatted images of MDCT scans obtained at 60.mAs (A) and 40 mAs (B) showing the pathological process (arrow). This structure is clearly identified andcorrectly assessed in both the scans.

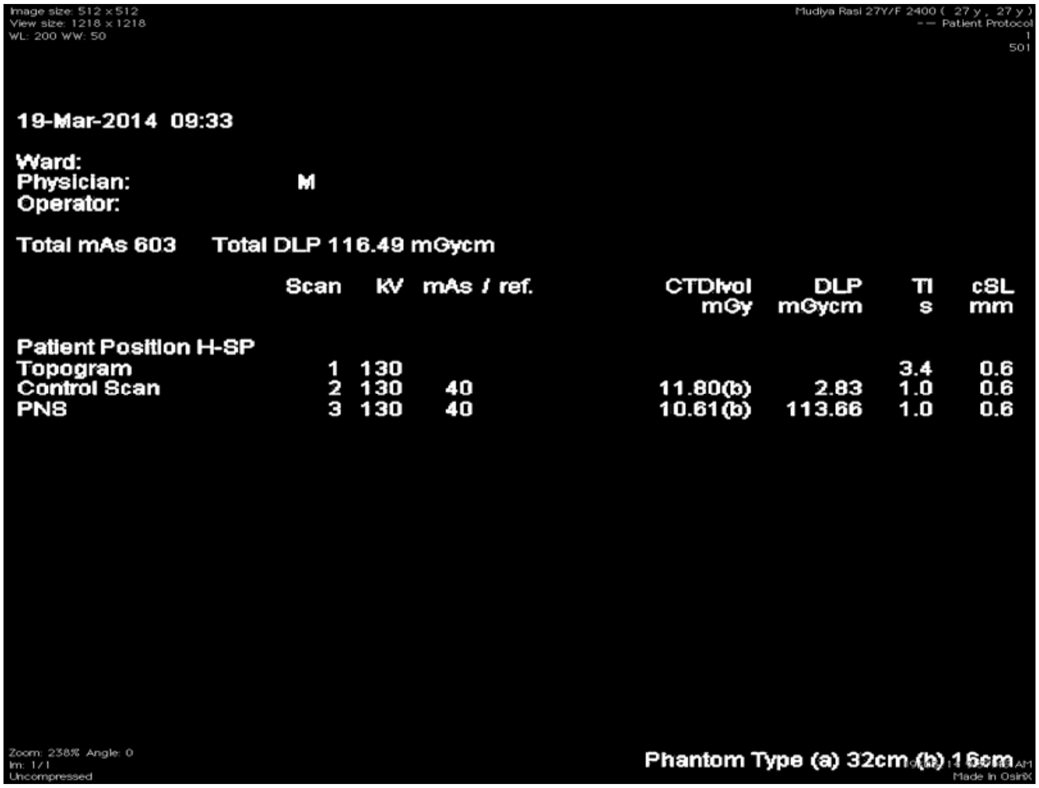

Image size: 512 x 512
View size: 1218 x 1218
WL: 200 WW: 50

Mudiya Rasi 27Y/F 2400 (27 y , 27 y)
-- Patient Protocol
1
501

19-Mar-2014 09:33

Ward:
Physician: M
Operator:

Total mAs 603 Total DLP 116.49 mGycm

	Scan	KV	mAs / ref.	CTDIvol mGy	DLP mGycm	TI s	cSL mm
Patient Position H-SP							
Topogram	1	130				3.4	0.6
Control Scan	2	130	40	11.80(b)	2.83	1.0	0.6
PNS	3	130	40	10.61(b)	113.66	1.0	0.6

Zoom: 238% Angle: 0
Im: 1/1
Uncompressed

Phantom Type (a) 32cm (b) 16cm
Made In OsiriX

Figure 13: CT generated dose chart showing the dose length product (DLP)

DISCUSSION

The role of CT scans for diagnosis of sinusitis has come a long way with advancements with CT imaging technology. It has been postulated that a high contrast difference between paranasal structures (bone, air and mucous membrane) should favour the use of low dose CT without significantly affecting the quality of images obtained. It is therefore possible to reduce CT dose without affecting diagnostic capability of CT scans for detection of sinusitis[30].

CT is the leading cause for medical radiation[40,41]. With increase in the amount of CT studies being conducted and the pace with which it is being increasingly employed it is but certain that background medical radiation will only increase. Therefore it is prudent that CT radiation dose be reduced wherever possible. Many studies are being conducted to assess whether reduction in CT radiation dose is possible without compromising on diagnostic quality of images.

Reducing exposure helps to reduce radiation received by the patient, improve economic viability, and also increase CT tube life[42]. While earlier studies involved higher mAs setting for evaluation of paranasal sinuses[42,43] recent studies have shown that low dose CT can be used without affecting sensitivity and specificity for evaluation of paranasal sinuses[30,33,44].

A similar study was conducted in UK, where in the authors evaluated the effect of reducing CT radiation dose on visualization of anatomical structures. It was a semi-quantitative study, which showed that CT scan of sinuses can be performed in patients at reduced CT dose without loss of diagnostic quality of images[30]. More recently researchers from Malaysia published results of their study in which 30 patients were evaluated with both low-dose and standard-dose CT technique. Their study strongly suggested that low-dose CT protocols should be employed for assessment of paranasal sinuses and associated pathologies[33].

Currently there are no standard parameters for a low-dose protocol. In one study, paranasal sinuses were evaluated using different mAs. It was concluded that except for evaluating bony landmarks, a low-dose CT technique involving as low as 16 mAs was sufficient to evaluate presence or abscence of sinusitis and to some extent the narrowing of ostia[45]. In a study conducted in 44 patients it was concluded that tube current setting of as low as 30 mAs was sufficient for evaluation of inflammatory disease of paranasal sinuses[36]. Furthermore, results from a study comparing 150 mAs and 10 mAs effective dose, showed that dose reduction had a far less important role to play when compared with human element of reviewer observation in detection of abnormalities. This was also associated with a radiation exposure of similar to that delivered by four view radiographic examination. The authors strongly suggested low-dose CT as method of choice for evaluation of sinusitis[31].

In the present study, all the paranasal sinuses were evaluated. The results showed that the maxillary sinus was the most commonly affected sinus followed by ethmoidal sinuses, which is not surprising given that these sinuses drain through the osteomeatal unit and are therefore commonly blocked[46]. These results reflect the findings observed elsewhere in other studies nationally and globally[47,48].

The current study did not find significant increase in noise when compared with other studies, which is not entirely unexpected given that those studies used very high mAs (100-200 mAs) as part of standard dose scan[30,33], while in the current study the standard dose was limited to 60 mAs. However, the current study was not powered or was designed to assess change in noise with lower mAs.

The current study showed that there was no statistically significant difference in terms of visualization of paranasal sinuses and pathologies with low-dose and standard-dose protocols. The results are in excellent agreement to the results published elsewhere with similar methodology. Both the studies used a similar semi-quantitative scoring methodology for description of anatomy or pathology. The results from both the studies did not show any statistically significant difference in terms of total score with standard-dose CT and low-dose CT. There was also an excellent inter-observer agreement in terms of structures visualized with both CT protocols[30,33]. In the current study there was no significant difference in the points scored for each of the anatomical structure or pathology with standard-dose and low-dose CT technique. In fact, barring infundibulum in one patient, where it was not clearly visualized, rest all the structures and pathologies were identified with no difference between the CT protocol arms. It is possible that in the hand of an experienced radiologist, even this discrepancy may not have crept in.

Our study compared the effect of tube current reduction by only 20 mAs, where as other studies have employed a much significant reduction in effective tube current[30,31,33].

Our study has few limitations. The patients were sequentially divided to receive either standard-dose or low-dose CT. Although analysis of low-dose and standard-dose findings in the same patient would have been ideal, it was not employed considering that it would be unethical to subject him/her for two scans. Paranasal structures are in close proximity to eye and this may increase risk of cataracts[28]. Secondly we did not make of use thermoluminescent dosimetry (TLD), which would have been a better choice for measurement of radiation dose[49,50]. Nevertheless we used CTDI and DLP to calculate the effective dose[25]. The patient population used in our study was limited to 60 and therefore these results may not be extrapolated to general population. However, the results of this study should pave way for further studies involving larger sample, particularly in Indian population. Moreover, the study was restricted for evaluation of visualization of normal anatomy and pathology in sinusitis and therefore the results may not be applicable when evaluating for malignancies[30]. Being a non-contrast study, the results may not apply for contrast enhanced scans as iodine-based contrasts may require different CT parameters[33,51].

It is well known that dose settings differ across different machines. To that effect it may not be possible to exactly use the same results from different CT scanners. However, the results can be applied to machines of similar make. The choice of CT dose settings also depends on the reading radiologist and institutional preferences. There is however sufficient evidence now to suggest that CT dose reduction is possible without affecting the diagnostic quality of scans and therefore this should be the current strategy across all centers/institutions.

To the best of our knowledge there are no studies conducted among Indians to evaluate the effect of low-dose CT for diagnosis of sinusitis. The current study was designed to evaluate anatomical structures and pathologies using low-dose CT. The current study employed methodology similar to that employed by other authors who used a semi-quantitative scoring methodology to assess visualization of anatomic structures and pathologies and a comparison was drawn from the responses. [30,33]. With the use of low-dose CT in this study, there was reduction in radiation received by the patient, reducing both medical radiation and background radiation. Although the study had some limitations, it nonetheless suggests that low-dose CT is not inferior to standard-dose CT for evaluation of sinusitis. These results have prompted the institution to consider revising the current CT protocol to include low-dose CT as routine protocol for evaluation of sinusitis. The same results may also be extrapolated to Indian population.

CONCLUSION

The maxillary sinus was the most common sinus involved across both the study groups followed by ethmoidal sinus.

There was no significant difference in the points scored for each of the anatomical structure or pathology with standard-dose and low-dose CT protocol. In fact, barring infundibulum in one patient, all the structures and pathologies were identified with no difference between both the CT protocol arms. The difference in image quality assessment was not statistically significant.

The mean radiation dose in low dose group was 0.26 mSv as compared to 0.38 mSv in the regular dose group resulting in more than 30% reduction in radiation dose to the patient.

The current study successfully demonstrated efficacy of low-dose protocol when compared to the standard dose protocol which is currently followed at our institute. We believe that despite the limitations with the current study, the results strongly support the role of low-dose CT for evaluation of clinically suspected sinusitis. Thus low dose CT protocol can be used as a routine examination in evaluation of sinusitis.

SUMMARY

Sinusitis is one of the most common health care problems worldwide and there is evidence that it is increasing in prevalence.Computed tomography (CT) is the gold standard for radiologic examination in the diagnosis and grading the severity of sinusitis. Limiting and reducing the radiation exposure is important, especially in young patients and in those who require repeated scanning. There is a considerable potential for reducing radiation dose in CT of the paranasal sinuses.

The aims of the study were to study the image quality of low-dose and regular dose MDCT scanning of the paranasal sinuses and compare the radiation dose.

The prospective study was carried out in 60 patients with clinically suspected paranasal sinusitis from January 2013 to June 2014 in the department of radio diagnosis of R L Jalappa hospital and research Centre, Tamaka, Kolar.

Alternate patients were taken up for low dose MDCT (130 kV and 40 mAs) and standard dose MDCT (130 kV and 60 mAs) of the paranasal sinuses with SIEMENS SOMATOM EMOTION 16 CT scanner.Diagnostic image quality was assessed by scoring for six anatomical structures and visualization of pathological processes. For each structure score was allocated as 0 if not demonstrated, 1 if demonstrated but not clearly visualized and 2 if clearly visualized. Effective dose was calculated by multiplying the dose length product with a factor of 0.0023.

Baseline demographic data was similar across both the groups. The maxillary sinus was the most common sinus involved across both the study groups (86.7% each) followed by ethmoidal sinus (66.7% and 56.7% in groups A and B). In the low dose group, 29 patients had a score of 14 compared with all patients (n = 30) in the regular dose group. Only one patient had a score of 13 in low-dose group. However, the difference was not statistically significant (P = 0.492).Mean effective dose in low-dose group was 0.26 mSv and 0.38 mSv in regular-dose group.

The mean radiation dose in low dose group was 0.26 mSv as compared to 0.38 mSv in the regular dose group, resulting in about 31% reduction in effective dose.

The study showed no statistically significant difference in terms of visualization of paranasal sinuses and pathologies with low-dose and standard-dose protocols. There was no significant difference in the points scored for each of the anatomical structure or pathology with standard-dose and low-dose CT technique. In fact, barring infundibulum in one patient, all the structures and pathologies were identified with no difference between the CT protocol arms.

The results of the study strongly support the role of low-dose CT in evaluation of clinically suspected sinusitis.

BIBLIOGRAPHY

1. Fokkens W, Lund V, Mullol J. European position paper on rhinosinusitis and nasal polyps. Rhinol2007:(Suppl 20)1-136.
2. Czechowski J, Janeczek J, Kelly G,Johansen J, Radiation dose to the lens in sequential and spiral CT of the facial bones and sinuses.EurRadiol 2001; 11(4): 711-3.
3. Kennedy DW, Zinreich SJ. The functional endoscopic approach toinflammatory sinus disease: current perspectives and techniquemodifications. Am J Rhinol 1988;2:89-93.
4. Zinreich S. Paranasal sinus imaging.Otolaryngol Head Neck Surg 1990;103:863-868.
5. Zinreich S. Imaging of inflammatory sinus disease.OtolaryngolClinNorth Am 1993;26:535-547.
6. How-Ming T, Vincent F H C. CT of the paranasal sinuses: normal anatomy, variants and pathology. CME Radiology 2001;2(3):120-125.
7. Bent JP, Cuilty-Siller C, Kuhn FA. The frontal cell as a cause of frontal sinus obstruction. Am J Rhinol 1994;8:185-191.
8. Landsberg, Roee, Friedman, Michael. A Computer-Assisted Anatomical Study of the Nasofrontal Region. Laryngoscope 2001;111(12):2125-2130.
9. Kasper KA. Nasofrontal connections. A study based on one hundred consecutive dissections. Arch Otolaryngol 1936;23: 322-343.

10. Gladwin V, Bhuvaneswari V and Ramachandra Rao K. Surgical Significance Of Sphenoidal And Ethmoidal Air Sinuses – By Coronal And Axial CT. Journal of the Anatomical Society of India 2007;56(1).

11. Zinreich S, Abidin M, Kennedy D. Cross-sectional imaging of the nasal cavity and paranasal sinuses. Operative Techniques OtolaryngolHeadNeckSurg 1990;1:93-99.

12. Yousem D. Imaging of sinonasal inflammatory disease. Radiology.1993;188:303-314.

13. Akif I, Yldrm A. B, Metin B, Muzaffer K. Ethmomaxillary sinus: a particular anatomic variation of the paranasal sinuses. Journal European Radiology. 2004;14(2):281-285.

14. Heinz R S, David W K Y. Paranasal Sinuses: Anatomic Terminology and Nomenclature. Adopted from Annals of Otology, Rhinology and Laryngology 1995;104:7-16.

15. Lindaek M, Johnsen U L H, Kaastad E, Dolvik S, Moll P, LaerumE,Jortdahl P. CT findings in general practice patients with suspected acutesinusitis. Actaradiologica 1996;37:(5)708-713.

16. Babbel R, Harnsberger H, Sonkens J, et al. Recurring patterns of inflammatory sinonasal disease demonstrated on screening sinus CT. Am J Neuroradiol 1992;13:903-912.

17. Sreeram E, ‘’ Computed Tomography: Physical Principles, Clinical applications and quality Control’’, 2nd edition, Philadelphia, USA: W.B. Saunders, 2001,7-12pp.

18. Bushberg JT, Seibert JA, Leidholdt EM, Boone JM. The essential physics of medical imaging. 2nd ed. Philadelphia, Pa: Lippincott Williams & Wilkins, 2001.

19. Rehani MM, Bongartz G, Kalender W, et al. Managing x-ray dose in computed tomography: ICRP Special Task Force report. Ann ICRP 2000; 30:7–45.

20. Mahesh M, Scatarige JC, Cooper J, Fishman EK. Dose and pitch relationship for a particular multislice CT scanner. AJR Am J Roentgenol 2001; 177:1273–1275.

21. Toth TL. Dose reduction opportunities for CT scanners.PediatrRadiol 2002; 32: 261–267.

22. Hu H, Fox SH. The effect of helical pitch and beam collimation on the lesion contrast and slice profile in helical CT imaging. Med Phys 1996; 23:1943–1954.

23. International Council on Radiation Protection.1990 recommendations of the International Commission on Radiological Protection.Publication 60, Annals of the ICRP 1991; 21. Oxford, England: Pergamon, 1991.

24. European Guidelines on Quality Criteria for Computed Tomography (EUR 16262 EN, May 1999) [internet]. [cited 2014 Oct 20]. Available from: www.drs.dk/guidelines/ct/quality/index.htm.

25. Jessen KA, Shrimpton PC, Geleijns J, Panzer W, Tois G. Dosimetry for optimisation of patient protection in computed tomography.ApplRadiatIsot 1999; 50:165–172.

26. Lund VJ, Lloyd DS, Lloyd G. Imaging for endoscopic sinus surgery in adults J Laryngol Otol. 2000 May;114(5):395-7.

27. Som PM. CT of the paranasal sinuses Neuroradiology (1985); 27:189-201.

28. Zammit-Maempel I, Chadwick CL, Willis SP. Radiation dose to the lens of eye and thyroid gland in paranasal sinus multislice CT. Br J Radiol 2003; 76(906):418-20.

29. Kalra M K, Maher M M, Toth TL, Hamberg LM, Blake MA, Shepard JA et al.Strategies for CT Radiation Dose Optimization. Radiology 2004; 230:619–628.

30. Sohaib S A, Peppercorn P D, Horrocks J D, Keene M H, Kenyon G S, Reznek R H. The effect of decreasing mAs on image quality and patient dose in sinus CT. The British Journal of Radiology, 74 (2001), 157–161.

31. Tack D, Widelec J, Maertelaer V, Bailly J M, Delcour C, Gevenois P A. Comparison Between Low-Dose and Standard-Dose Multidetector CT in Patients with Suspected Chronic Sinusitis.AJR2003;181:939–944.

32. Kasim K A, Strömbeck A, Johnson P S. Low- dose computed tomography of the paranasal sinuses: radiation doses and reliability analysis. American Journal of Otolaryngology–Head and Neck Medicine and Surgery 32 (2011) 47–51.

33. Lam S, Bux S, Kumar G, Ng Kh, Hussain A. A comparison between low-dose and standard-dose non-contrasted multidetector CT scanning of the paranasal sinuses. Biomed Imaging Interv J 2009 Jul;5(3):e13.

34. Hojreh A, Czerny C, Kainberger F. Dose classification scheme for computed tomography of the paranasal sinuses. Eur J Radiol 2005 Oct;56(1):31-7.

35. Akayleh R. Comparison of low and high computed tomography radiation dose in sinusitis. Hard Tissue 2014 Feb 10;3(1):4.

36. Duvoisin B, Landry M, Chapuis L, Krayenbuhl M, Schnyder P. Low-dose CT and inflammatory disease of the paranasal sinuses. Neuroradiology 1991;33(5):403-6.

37. Hagtvedt T, Aalokken TM, Notthellen J, Kolbenstvedt A, Haye R. Sinus radiography and low-dose CT in the diagnosis of acute sinusitis. Tidsskr Nor Laegeforen 2003 Dec 4;123(23):3362-4.

38. Hagtvedt T, Aaløkken TM, Nøtthellen J, Kolbenstvedt A. A new low-dose CT examination compared with standard-dose CT in the diagnosis of acute sinusitis. EurRadiol 2003 May;13(5):976-80.

39. Bulla S, Blanke P, Hassepass F, Krauss T, Winterer JT, Breunig C, et al. Reducing the radiation dose for low-dose CT of the paranasal sinuses using iterative reconstruction: feasibility and image quality. Eur J Radiol 2012 Sep;81(9):2246-50.

40. Semelka RC, Armao DM, Elias J Jr, Huda W. Imaging strategies to reduce the risk of radiation in CT studies, including selective substitution with MRI. J MagnReson Imaging 2007 May;25(5):900-9.

41. Frush DP, Donnelly LF, Rosen NS. Computed tomography and radiation risks: what pediatric health care providers should know. Pediatrics 2003 Oct;112(4):951-7.

42. Babbel R, Harnsberger HR, Nelson B, SonkensJ,Hunt S. Optimization of techniques in screening CTof the sinuses. Am J Neuroradiol 1991;12:849–54.

43. Rowe-Jones J, Mackay I, Colquhoun I. Charing Cross CT protocol for endoscopic sinus surgery. J LaryngolOtol 1995;109:1057–60.

44. Kearney SE, Jones P, Meakin K, Garvey CJ. CT scanning of the paranasal sinuses—the effect of reducing mAs. Br J Radiol 1997;70:1071–4.

45. Marmolya G, Wiesen EJ, Yagan R, Haria CD, Shah AC. Paranasal sinuses: low-dose CT. Radiology 1991 Dec;181(3):689-91.

46. Hamilos DL. Chronic sinusitis. J Allergy ClinImmunol 2000 Aug;106(2):213-27.

47. Scaria ST, Bhandary SK, Rajeshwary A, Bhat VS. Radiological evidence of frequency of involvement of paranasal sinuses in chronic rhinosinusitis. J Med Health Sci 2014;3(2):118-21.

48. Nair S. Correlation between symptoms and radiological findings in patients of chronic rhinosinusitis: a modified radiological typing system. Rhinology 47,181-186, 2009.

49. Oliveira ML, Maia AF, Nascimento NC, Fragoso MC, GAlindo RS, Hazin CA. Influence of thermoluminescent dosimeters energy dependence on the measurement of entrance skin dose in radiographic procedures.Radiol Bras 2010 Mar-Apr;43(2):113–8.

50. Tootell AK, Szczepura KR, Hogg P. Optimising the number of thermoluminescent dosimeters required for the measurement of effective dose for computed tomography attenuation correction data in SPECT/CT myocardial perfusion imaging. Radiography 2013;19(1):42-7.

51. McCollough CH1, Primak AN, Braun N, Kofler J, Yu L, Christner J. Strategies for reducing radiation dose in CT. RadiolClin North Am 2009 Jan;47(1):27-40.

ANNEXURES

CASE PROFORMA

Name:

Age:

Sex:

Hospital number:

Presenting complaints:

Paranasal sinus involvement:

Frontal sinus	Ethmoid sinus	Maxillary sinus	Sphenoid sinus

Image quality assessment criteria:

Criteria	0	1	2
Osteomeatal unit			
Uncinate process			
Infundibulum			
Frontal recess			
Attachments of the middle turbinate			
Path of the optic nerve			
Pathological changes			

Total (Max 14) –

Effective dose (mSv) –

INFORMED CONSENT FORM

I, Mr/Miss/Mrs____,

have been invited to participate in project titled “A comparison between low-dose and standard dose non-contrast multidetector computed tomographic imaging in inflammatory diseases of paranasal sinuses”. It has been communicated to me in my vernacular language about the purpose of the study and the associated possible complications.

My participation in this research project is purely voluntary. I am also aware that I can withdraw from the project at any point of time without citing any reasons whatsoever.

I also agree to co-operate with him and agree by my own free will and in complete consciousness without any influence hereby I give my consent.

Name and Signature/thumbprint.

MASTER CHART

S.No.	Name	Age	Sex	Tube current (mAs)	Sinus involved				Image quality assessment																					Total (Max - 14)	Effective dose (mSv)
									Maxillary ostium			Uncinate process			Infundibulum			Frontal recess			Attachments of middle turbinates			Pathway of optic nerve			Pathological changes				
					Frontal	EThmoid	Maxillary	Sphenoid	0	1	2	0	1	2	0	1	2	0	1	2	0	1	2	0	1	2	0	1	2		
1	Yakobu	37	M	40	-	+	+	-	-	-	+	-	-	+	-	-	+	-	-	+	-	-	+	-	-	+	-	-	+	14	0.25
2	Shiva	18	M	60	+	+	+	+	-	-	+	-	-	+	-	-	+	-	-	+	-	-	+	-	-	+	-	-	+	14	0.37
3	Sanjay	30	M	40	+	+	+	+	-	-	+	-	-	+	-	-	+	-	-	+	-	-	+	-	-	+	-	-	+	14	0.31
4	Merulappa	50	M	60	-	-	+	-	-	-	+	-	-	+	-	-	+	-	-	+	-	-	+	-	-	+	-	-	+	14	0.42
5	Akshita	19	F	40	-	+	-	-	-	-	+	-	-	+	-	-	+	-	-	+	-	-	+	-	-	+	-	-	+	14	0.25
6	Merulappa	50	M	60	-	-	+	-	-	-	+	-	-	+	-	-	+	-	-	+	-	-	+	-	-	+	-	-	+	14	0.42
7	Balamma	55	F	40	-	-	+	+	-	-	+	-	-	+	-	-	+	-	-	+	-	-	+	-	-	+	-	-	+	14	0.26
8	Afzal pasha	18	M	60	-	+	+	-	-	-	+	-	-	+	-	-	+	-	-	+	-	-	+	-	-	+	-	-	+	14	0.42
9	Sundaresan	72	M	40	+	+	+	+	-	-	+	-	-	+	-	-	+	-	-	+	-	-	+	-	-	+	-	-	+	14	0.27
10	ZameenTaj	44	M	60	-	-	+	-	-	-	+	-	-	+	-	-	+	-	-	+	-	-	+	-	-	+	-	-	+	14	0.35
11	Nirmala	62	F	40	-	-	+	+	-	-	+	-	-	+	-	-	+	-	-	+	-	-	+	-	-	+	-	-	+	14	0.26
12	Shafiya	23	F	60	+	+	+	+	-	-	+	-	-	+	-	-	+	-	-	+	-	-	+	-	-	+	-	-	+	14	0.37
13	Chotesab	50	M	40	-	-	+	-	-	-	+	-	-	+	-	-	+	-	-	+	-	-	+	-	-	+	-	-	+	14	0.25
14	Savitha	23	F	60	-	-	+	-	-	-	+	-	-	+	-	-	+	-	-	+	-	-	+	-	-	+	-	-	+	14	0.36
15	Nirmala	50	F	40	-	+	+	-	-	-	+	-	-	+	-	-	+	-	-	+	-	-	+	-	-	+	-	-	+	14	0.24
16	Sampath Kumar	52	M	60	-	+	+	-	-	-	+	-	-	+	-	-	+	-	-	+	-	-	+	-	-	+	-	-	+	14	0.37
17	RaziyaFirdouze	27	F	40	-	+	+	-	-	-	+	-	-	+	-	-	+	-	-	+	-	-	+	-	-	+	-	-	+	14	0.24
18	Lini Mathew	21	F	60	-	-	+	-	-	-	+	-	-	+	-	-	+	-	-	+	-	-	+	-	-	+	-	-	+	14	0.38
19	Roopa	28	F	40	-	-	+	-	-	-	+	-	-	+	-	-	+	-	-	+	-	-	+	-	-	+	-	-	+	14	0.25

MASTER CHART

20	Muniyappa	63	M	60	-	-	+	-	-	-	+	-	-	+	-	-	+	-	-	+	-	-	+	-	-	+	-	-	+	14	0.39
21	Ambirish	42	M	40	-	+	+	-	-	-	+	-	-	+	-	-	+	-	-	+	-	-	+	-	-	+	-	-	+	14	0.28
22	Manjunath	34	M	60	+	+	+	-	-	-	+	-	-	+	-	-	+	-	-	+	-	-	+	-	-	+	-	-	+	14	0.47
23	Srinath	34	M	40	-	-	+	-	-	-	+	-	-	+	-	-	+	-	-	+	-	-	+	-	-	+	-	-	+	14	0.25
24	Manjula	25	F	60	+	+	+	+	-	-	+	-	-	+	-	-	+	-	-	+	-	-	+	-	-	+	-	-	+	14	0.37
25	Vennila	32	F	40	-	+	-	+	-	-	+	-	-	+	-	-	+	-	-	+	-	-	+	-	-	+	-	-	+	14	0.25
26	Nandhish	25	M	60	-	+	+	-	-	-	+	-	-	+	-	-	+	-	-	+	-	-	+	-	-	+	-	-	+	14	0.38
27	Narayanaswamy	57	M	40	+	+	+	+	-	-	+	-	-	+	-	-	+	-	-	+	-	-	+	-	-	+	-	-	+	14	0.25
28	Kalpana	24	F	60	+	+	+	+	-	-	+	-	-	+	-	-	+	-	-	+	-	-	+	-	-	+	-	-	+	14	0.38
29	Geethabai	44	F	40	+	+	+	+	-	-	+	-	-	+	-	+	-	-	-	+	-	-	+	-	-	+	-	-	+	13	0.25
30	Gopal Gowda	63	M	60	+	+	+	+	-	-	+	-	-	+	-	-	+	-	-	+	-	-	+	-	-	+	-	-	+	14	0.4
31	Muniraj	30	M	40	-	+	+	-	-	-	+	-	-	+	-	-	+	-	-	+	-	-	+	-	-	+	-	-	+	14	0.25
32	Arun Kumar	19	M	60	-	-	+	-	-	-	+	-	-	+	-	-	+	-	-	+	-	-	+	-	-	+	-	-	+	14	0.39
33	DivyaBharathi	19	F	40	+	+	+	+	-	-	+	-	-	+	-	+	+	-	-	+	-	-	+	-	-	+	-	-	+	13	0.29
34	Anitha	37	F	60	-	+	-	-	-	-	+	-	-	+	-	-	+	-	-	+	-	-	+	-	-	+	-	-	+	14	0.39
35	Mahesh	30	M	40	-	+	+	+	-	-	+	-	-	+	-	-	+	-	-	+	-	-	+	-	-	+	-	-	+	14	0.28
36	Abhishek	18	M	60	+	+	+	-	-	-	+	-	-	+	-	-	+	-	-	+	-	-	+	-	-	+	-	-	+	14	0.47
37	Preethy	18	F	40	-	-	+	-	-	-	+	-	-	+	-	-	+	-	-	+	-	-	+	-	-	+	-	-	+	14	0.25
38	Chinappa	34	M	60	-	+	+	-	-	-	+	-	-	+	-	-	+	-	-	+	-	-	+	-	-	+	-	-	+	14	0.41
39	Sanjeeva Kumar	49	M	40	+	-	-	-	-	-	+	-	-	+	-	-	+	-	-	+	-	-	+	-	-	+	-	-	+	14	0.27
40	Parvathamma	55	F	60	-	-	+	-	-	-	+	-	-	+	-	-	+	-	-	+	-	-	+	-	-	+	-	-	+	14	0.4
41	Vamsi Reddy	19	M	40	+	-	+	-	-	-	+	-	-	+	-	-	+	-	-	+	-	-	+	-	-	+	-	-	+	14	0.26

MASTER CHART

42	Munipillapa	38	M	60	+	+	+	-	-	-	+	-	-	+	-	-	+	-	-	+	-	-	+	-	-	+	-	-	+	14	0.42
43	Bhavani	29	F	40	+	+	+	-	-	-	+	-	-	+	-	-	+	-	-	+	-	-	+	-	-	+	-	-	+	14	0.24
44	Chaitra	28	F	60	-	+	+	-	-	-	+	-	-	+	-	-	+	-	-	+	-	-	+	-	-	+	-	-	+	14	0.39
45	Shylu	23	F	40	-	-	+	+	-	-	+	-	-	+	-	-	+	-	-	+	-	-	+	-	-	+	-	-	+	14	0.28
46	Puttegowda	42	M	60	+	+	-	-	-	-	+	-	-	+	-	-	+	-	-	+	-	-	+	-	-	+	-	-	+	14	0.43
47	Sakamma	35	F	40	+	-	-	-	-	-	+	-	-	+	-	-	+	-	-	+	-	-	+	-	-	+	-	-	+	14	0.24
48	Padmamma	49	F	60	-	+	+	+	-	-	+	-	-	+	-	-	+	-	-	+	-	-	+	-	-	+	-	-	+	14	0.4
49	Mudiyarasi	27	F	40	-	-	+	-	-	-	+	-	-	+	-	-	+	-	-	+	-	-	+	-	-	+	-	-	+	14	0.26
50	Rekha	31	F	60	-	-	+	-	-	-	+	-	-	+	-	-	+	-	-	+	-	-	+	-	-	+	-	-	+	14	0.41
51	Marappa	66	M	40	-	+	+	-	-	-	+	-	-	+	-	-	+	-	-	+	-	-	+	-	-	+	-	-	+	14	0.27
52	Shreyas	28	M	60	+	+	+	+	-	-	+	-	-	+	-	-	+	-	-	+	-	-	+	-	-	+	-	-	+	14	0.4
53	Sujatha	27	F	40	-	-	+	-	-	-	+	-	-	+	-	-	+	-	-	+	-	-	+	-	-	+	-	-	+	14	0.23
54	Munireddy	38	M	60	-	+	+	-	-	-	+	-	-	+	-	-	+	-	-	+	-	-	+	-	-	+	-	-	+	14	0.43
55	Mageshwari	29	F	40	+	+	+	+	-	-	+	-	-	+	-	-	+	-	-	+	-	-	+	-	-	+	-	-	+	14	0.25
56	Venkatamma	45	F	60	-	+	-	-	-	-	+	-	-	+	-	-	+	-	-	+	-	-	+	-	-	+	-	-	+	14	0.39
57	Harish	19	M	40	-	+	+	-	-	-	+	-	-	+	-	-	+	-	-	+	-	-	+	-	-	+	-	-	+	14	0.27
58	Mohammed Ali	24	M	60	-	+	+	-	-	-	+	-	-	+	-	-	+	-	-	+	-	-	+	-	-	+	-	-	+	14	0.42
59	Rajakumar	30	M	40	-	-	+	-	-	-	+	-	-	+	-	-	+	-	-	+	-	-	+	-	-	+	-	-	+	14	0.23
60	Fathima Begum	29	M	60	-	-	+	-	-	-	+	-	-	+	-	-	+	-	-	+	-	-	+	-	-	+	-	-	+	14	0.4